RADC-TDR-62-286

62-4-5

16 May 1962

ELECTRICAL BREAKDOWN IN THE ATMOSPHERE

by

A. D. MacDonald
H. W. Bandel, D. U. Gaskell, H. N. Gitterman

FINAL REPORT

Contract No. AF 30(602)-2501

Prepared for

Rome Air Development Center
Air Force Systems Command
United States Air Force

Griffiss Air Force Base
New York

PALO ALTO LABORATORIES
MICROWAVE PHYSICS LABORATORY

GENERAL TELEPHONE AND ELECTRONICS LABORATORIES, INC.

ELECTRICAL BREAKDOWN IN THE ATMOSPHERE

by

A. D. MacDonald
H. W. Bandel, D. U. Gaskell, H. N. Gitterman

GENERAL TELEPHONE AND ELECTRONICS LABORATORIES, INC.
MICROWAVE PHYSICS LABORATORY
1015 Corporation Way
Palo Alto, California

FINAL REPORT

Contract No. AF 30(602)-2501

Project No. 5561
Task No. 55237

Prepared for

Rome Air Development Center
Air Force Systems Command
United States Air Force

Griffiss Air Force Base
New York

FOREWORD

The trend of radar design is such that in the foreseeable future the rf energy transmitted into space will be of sufficient magnitude to cause concern over the ability of the atmosphere to support this transmission. Transmission of peak powers in the order of 20 Mw and greater have been reported in the literature. Multiple element arrays (phased arrays) are capable of summing the energies of several transmitters. Radars of this type have been designed for transmission of peak powers of 150 Mw. Single element transmitters for such arrays are capable of power generation in the order of 100 kw, suggesting a boundless design limit on the transmitted energy. Such energy transmission is limited only by the number of elements, element spacing, the geometry of the surveillance volume, and the ability of the atmosphere to support the transmitted energy. A definition of the limits placed on the amount of transmitted energy to be supported by atmosphere is of immediate concern and is the subject of the work reported.

Theoretical and experimental investigations have been carried out by both commercial and Government laboratories during the past several years, using various noble gases and air as transmission media. Experiments are generally of two types--those conducted in waveguides and resonant cavities and those conducted in non-resonant containers. The experimental technique using waveguides permits a clear delineation of the electric field; however, electron diffusion

to the walls of the waveguide affects the results. The use of large non-resonant cavities minimizes these effects; however, the electric field distribution is difficult to describe. The approach taken in this work uses the waveguide technique at L-, X-, and K-band, with both pulsed and cw power.

A sufficiently wide range of atmospheric conditions has been simulated such that the results obtained and presented in graphical form in this report can be used to predict the effective field strengths for the threshold of breakdown in the frequency region for 100 Mc/s to 100 kMc/s to altitudes of 100 km.

Further work in the area of atmospheric breakdown is being directed toward the problem of evaluating the limits on transmission in the region of breakdown.

ABSTRACT

This report contains the results of experiments on breakdown electric fields at L-, X-, and K-band over a large pressure range and in a large number of resonant cavities of different sizes. Progress in the beam-type experiments designed to measure attachment and collision cross-sections at very low energies is described. A method of using the experimental data to predict breakdown fields under both pulsed and cw conditions is described. It is considered unlikely that further experimental data on electrical breakdown in the atmosphere at pressures ranging from atmospheric to that at 100 km altitude, and in the frequency range of 100 Mc/s to 100 kMc/s, would lead to conclusions different from those contained in this report.

TABLE OF CONTENTS

LIST OF ILLUSTRATIONS

ELECTRICAL BREAKDOWN IN THE ATMOSPHERE

INTRODUCTION.

The object of the work supported by Contract AF 30(602)-2501 and its predecessor, AF 30(602)-2261, was to discover the electric fields and powers required to initiate electrical breakdown in the atmosphere for a number of different frequencies and for a variety of altitudes. In order to determine these, we set up a program of measurements of breakdown electric fields in resonant microwave cavities at three different frequencies (1, 9.4, and 24 kMc/s) and also a program of measurements of collision and attachment cross-sections for the atmospheric gases. The detailed considerations which led to this experimental program are contained in Scientific Report No. 1[1] and the Final Report of May, 1961.[2]

This report will not include all of the theoretical considerations and calculations which are included in the previous reports, but we will present here detailed information on experiments at L-, X-, and K-band, both pulsed and cw, for a very wide variation of pressure and for a large number of individual resonant cavities.

Section A contains the detailed information on the experimental arrangements and the experimental results, as well as theoretical considerations and a scheme for calculating breakdown in the atmosphere, for a wide range of conditions likely to be met at high altitudes.

Section B contains a description of the work undertaken to measure the collision cross-sections and the attachment cross-sections for atmospheric gases. Both of these processes are important in determining breakdown electric fields and powers; and although we have not yet made any measurements by the beam technique, considerable progress toward this goal has been made.

A. MICROWAVE BREAKDOWN IN AIR, NITROGEN, AND OXYGEN.

1. General Considerations.

When the experimental program for measuring microwave breakdown fields in the air and in the atmospheric gases was set up in the Microwave Physics Laboratory, there existed very little experimental information. There had been a number of theoretical studies, but the experimental work of Herlin and Brown,[3] of Rose and Brown,[4] and of Gould and Roberts[5] provided the only measurements, and these did not cover a very wide range of variation of experimental parameters. Although the theoretical analyses based on solutions of the Boltzmann equation and kinetic theory calculations had shown remarkable agreement with experiment for both helium and hydrogen and had made possible predictions of breakdown electric fields over extremely wide variations of frequency and pressure, similar calculations were not possible for air. The simplifications in the Boltzmann equation resulting from the energy variation in the collision cross-sections of helium and hydrogen cannot be used in dealing with air.

Such theoretical calculations as had been made in air had used the idea of an effective electric field. This idea of an effective electric field may be shown to be very useful when the electron-neutral particle collision cross-sections are such that the collision frequency is independent of energy, and it is perhaps in order at this time to explain in some detail the concept of an effective electric field.

When a high frequency electric field is applied across a gas containing a few electrons, the electrons are accelerated; and if the collision frequency is very much higher than the frequency of the applied field, the energy which the electrons gain from the electric field is proportional to the electric field multiplied by the mean free path. Phase relationships between the field and the electron motion are disrupted by collisions, and so the field acts, in effect, like a dc field. On the other hand, when the pressure is so low that the collision frequency is very much lower than the frequency of the applied field, the electrons tend to oscillate out of phase with the electric field; and, therefore, under this situation the energy transfer is relatively low. The formulation of the effective electric field is an attempt to put these ideas in a quantitative fashion in order to make numerical calculations.

The most useful such calculation can be taken from a study of the Boltzmann equation. The Boltzmann equation is a differential equation for the electron energy distribution function, in terms of the experimental parameters, with the electron energy as the

independent variable. For the purposes of this section we may write the Boltzmann equation in the following manner:

$$E^2 \Lambda^2 \nu \frac{d}{du}\left[u^{3/2} \frac{\nu}{\nu^2 + \omega^2} \frac{df}{du}\right] + \alpha \Lambda^2 \nu \frac{d}{du}(\nu u^{3/2} f) - u^{3/2} f = 0, \qquad (1)$$

where f is the distribution function; u is equal to $mv^2/2e$ and is the measure of the energy of the electrons in terms of volts; ν is the electron-neutral particle collision frequency; ω is 2π times the frequency of the applied field. Λ is the characteristic diffusion length, which is a measure of the size of the container in which the breakdown is taking place, and which, for example, for the case of parallel plates separated by a distance L, is equal to L/π. α is a constant composed of the mass and charge of an electron, and the mass of the atoms. Terms involving inelastic collisions are omitted in Equation (1) because they do not alter the argument.

If ν is independent of the energy u, we can simplify this equation very readily in the following way:

$$E_e^2 \Lambda^2 \frac{d}{du}\left[u^{3/2} \frac{df}{du}\right] + \alpha \nu^2 \Lambda^2 \frac{d}{du}(u^{3/2} f) - u^{3/2} f = 0, \qquad (2)$$

where $E_e^2 = \frac{E^2}{\left[1 + (\omega^2/\nu^2)\right]}$. This defines the effective electric field; and inspection shows that for high pressure or low frequency E_e is equal to E, while for high frequencies the effective field is approximately $E(\nu/\omega)$. All of the experimental parameters are then included in the two quantities , $E_e \Lambda$ and $\nu \Lambda$, and so all breakdown phenomena for such

a case can be described by a single line representing the relationship between E_e/Λ and ν/Λ (or p/Λ, since ν is directly proportional to p).

We can see from Figure 1 that in the case of air the collision frequency is not at all independent of energy; and, therefore, this particular simplification cannot necessarily be made. This means that all of the breakdown data for a variety of pressures and frequencies may not be representable by a single curve in two dimensions, and it may be necessary to represent breakdown by a family of curves or a surface in three dimensions. With these considerations in mind, and because of the difficulties of extrapolating earlier theoretical analyses, it was considered advisable to do experiments for a wide range of variation of frequency, of pressure, and of container size; and this was the basis upon which we set up the experimental program.

2. Experimental Arrangements.

The experimental arrangements which were used have been described in considerable detail in the reports referred to above.[1,2] A typical microwave system is shown schematically in Figure 2. Power, either pulsed or cw, from the magnetron oscillator, is monitored by the power meter and guided by a standard microwave circuit to the cavity which is being tested. The frequency is measured to a high degree of accuracy, and there are transmission and reflection meters to determine when breakdown has taken place. The details of the experimental

arrangements and the methods of calculating the electric field from the known incident power and the cavity properties have been described elsewhere.[1,2,3,6]

Although the methods of measurement are basically the same as those used in previous breakdown measurements, there are a number of specific points which should be noted. Measurements were made on ten different cavities of widely different properties, as described in Table 1. Power measurements were more accurate than those obtained earlier and the estimated accuracy of the cw fields is 2 percent, with repeatability of about 1 percent. The pulsed data are estimated to be accurate to about 10 percent for the short pulses and a little better for the long pulses. Fabrication of the cavities was complicated by the possiblities of reaction between the products of breakdown and the walls. All cavities were made of copper, plated or flashed with rhodium. All were made so that they could be baked as part of the vacuum system, although it was found that baking was not always necessary. We found it convenient to control the temperature of the cavities by water cooling so that resonant frequencies would not drift. Power was coupled to the cavities by loops at L-band and by irises at X- and K-bands.

A typical vacuum system is described schematically in Figure 3. A great deal of care was taken to use only pure gases; and it was found, as had been previously known from the work of Rose and Brown, that unless one used pure air and introduced new air by flushing out the system after each breakdown, incorrect results would

TABLE I

PROPERTIES OF MICROWAVE CAVITIES

Cavity	Mode	Radius (cm)	Height (cm)	λ (cm)	Frequency (kMc/s)	Pressure Range (mm Hg)
L1	TM_{010}	11.561	1.999	0.631	0.992	0.01 - 70
L2	TM_{010}	11.510	5.000	1.51	0.994	0.01 - 80
L3	TM_{010}	11.510	10.008	2.65	0.994	0.005 - 50
X10A	TM_{010}	1.222	0.330	0.103	9.33	0.1 - 150
X11A	TM_{010}	1.222	0.767	0.220	9.40	0.1 - 100
X13A	TM_{010}	1.222	2.040	0.400	9.40	0.1 - 120
X18A	TM_{030}	4.384	5.740	1.29	9.41	0.2 - 100
X19A	TM_{030}	4.384	2.184	0.65	9.40	0.2 - 100
X17A	TM_{230}	(4.912 x 6.353 x 6.985)		-	9.38	0.2 - 80
K1	TM_{010}	0.472	0.332	0.093	24.1	8.0 - 200

be obtained. The oil manometer in Figure 3 was replaced by a third McLeod gauge for most of the measurements. A detailed description of our vacuum system is contained in previous reports and will not be repeated here.

Pure dry air in one-litre Pyrex flasks was used for the air breakdown data presented in this report. We set up a purifying and drying system to enable us to use room air; and although it was found that with sufficient precautions this air would give results equal to those with the pure air, it was found to be less time-consuming to use the commercially prepared dry air. The measurements with nitrogen, oxygen, and hydrogen were also performed using commercially available spectroscopically pure gases in one-litre Pyrex flasks.

Measurements were made on three cavities of different sizes at L-band, at a frequency of 994 Mc/s, with characteristic diffusion lengths varying from 0.63 cm to 2.65 cm. CW measurements were made in air, in oxygen, and in nitrogen in all cavities and in hydrogen and some other gases in one cavity. Pulsed data were taken on one cavity in air and in nitrogen. Measurements were made on three cavities at X-band (9.4 kMc/s), operating in the lowest magnetic mode. Breakdown fields were measured in air in all cavities. Pulsed measurements were made in nitrogen and in air in two of these cavities. At this frequency there were also measurements made on two TM_{030} mode cavities and one cubical high mode cavity, operating in the TM_{230} mode. At a frequency of 24.1 kMc/s (K-band), measurements were made on one

cavity and these measurements were for pulsed power. The characteristic diffusion length in this case was .093 cm.

The experimental results at L-band are shown in Figures 4 through 11. The cw breakdown fields are shown as functions of pressure with the pressure varying from approximately .01 mm Hg to about fifty mm Hg, the limits being determined by the power available, as was the case with all of our measurements. These pressures correspond to altitudes ranging from approximately fifteen to eighty kilometers. Breakdown measurements for air and nitrogen are shown on all three cavities and for oxygen and hydrogen on two of them.

The departure of the air and the nitrogen curves from one another at the higher pressures is probably caused by attachment which takes place in the oxygen component of the air and probably not at all in nitrogen, and it is to be noted that the departure is somewhat greater for the larger cavities.

Figure 7 also shows the cw breakdown data for air plotted for all cavities on the same curve and shows the way in which the container size or characteristic diffusion length determines the breakdown field. It will be noted that at the higher pressures all cavities show essentially the same breakdown field, indicating that attachment is probably very largely responsible for the loss of electrons; whereas at the lower pressures there is a substantial difference between the results in the three different cavities,

indicating that the characteristic diffusion length is the important parameter and that the predominant electron removal mechanism is diffusion.

Breakdown data were also taken for pulsed power in one of the L-band cavities. These data are presented in two different ways. In Figure 9 is shown the cw breakdown curve for air, as well as some pulsed breakdown curves calculated from the theory which will be discussed later in this report. This pulsed breakdown field is that field required to initiate breakdown at the end of the pulse. The dashed lines are calculated and the individual points are the experimental results. These data are also shown for both air and nitrogen in a somewhat different manner in Figures 10 and 11. In these figures we have plotted the breakdown field as a function of pulse width for a number of different pressures. All of these pulse data were taken with the pulse repetition rate of 1000 per second. Repetition rate was also variable, and some data were taken with the pulse repetition rate of 100 per second, but this change produced no significant difference. This was taken to mean that for these particular conditions the ionization created in one pulse had sufficient time to decay before the next pulse arrived.

It was necessary to establish a criterion for breakdown for the pulsed measurements. We did this by considering the oscilloscope display of pulse shape of the power transmitted through the cavity. As the power was raised a point would be reached at which the height of the trailing edge of the pulse was sharply reduced.

This indicated that breakdown had taken place by the time the pulse ended. This method clearly made accurate measurements more difficult at short pulse lengths and it is to be noted that in all cases the agreement between measurements and calculations is worse at the short pulse lengths than for the longer pulses.

In order to get reproducible results for pulsed breakdown it is necessary that there be some electrons in the high field volume during the time of the pulse. We found it necessary to have a 5 millicurie cobalt-60 gamma-ray source next to the cavities to produce sufficient ionization to get repeatable results for the pulsed work although a 5 microcurie source had sufficed for the cw work.

Figures 12 through 15 show the cw breakdown data for air, nitrogen, and oxygen, and in some cases hydrogen, for the X-band cavities resonant in the lowest magnetic mode. Figures 16 and 17 show the data for two larger TM_{030} mode cavities. Figure 23 shows a series of curves for air breakdown in five cavities of different characteristic diffusion lengths. In Figures 18, 19, and 20 are shown the X-band pulsed data taken in the manner similar to that described above, and, also, in Figures 21 and 22 are shown the breakdown fields for pulsed data as a function of pulse width. The general character of these curves is very much like those at the lower frequency.

At a frequency of 24.1 kMc/s we have data on only one cavity. These data are presented in Figures 24 through 28. At this frequency we did not have available sufficiently powerful sources

to do any cw breakdown measurements. However, with the results of the work at lower frequencies we were able to correlate the pulsed and the cw data and so are able to predict quite accurate cw breakdown. The data are presented in some detail in these figures. The pressure range for which we have data corresponds to a range of altitude of approximately 10 to 40 kilometers. Obtaining data at this high frequency presented a number of difficulties which were not present in the lower frequency work. Because we did not have a tunable cw magnetron, we were not able to do any cw measurements; and because the magnetron which we had was tunable only over a very narrow range of frequency, the fabrication of the cavities presented very great difficulties. A change in the diameter of the cavities, for example, of a thousandth of an inch resulted in a resonant frequency change of about 40 Mc/s. This was about ten times the range over which the magnetron frequency could be tuned. Therefore, the construction of the cavities required very great care with dimensions. The cavities which had been constructed for the X-band and the L-band data were made of copper, nickel plated and then rhodium flashed to prevent reaction between the walls of the cavity and the gas after the breakdown takes place in air or in oxygen. It was found, however, that nickel could not be plated uniformly on the very small cavities. Various time-consuming methods were tried but it was found finally that a cavity could be made from copper with a nickel flash and then a rhodium flash which would not radically change the dimensions. The input and the output coupling irises also changed the frequency

somewhat, and this was used after the cavity had been assembled to do some final frequency adjustments. Temperature control was important and temperature variations were also used when necessary to tune the resonance of the cavity to that of the magnetron. The properties of the cavity were determined by a low powered cw tunable stable oscillator, and the magnetron used only for the breakdown measurements.

The experimental arrangements for K-band were similar to those at X-band and L-band. However, after the work was in progress it was found that the power divider could be done away with and a high power attenuator and a calibrated variable attenuator used instead. This resulted in some improvements in measuring technique. However, the accuracy of the K-band measurements is not comparable with that at X-band and L-band because the frequency is not as easily or as accurately measurable and the power level is not readily measurable to the high precision that is possible at the lower frequencies. The over-all accuracy of the K-band measurements is estimated at approximately ten percent.

3. Electron Diffusion in a High Mode Cavity.

There have been several studies of electron diffusion in cavities in which the non-uniform nature of the microwave electric field has complicated our understanding of the breakdown phenomena.[7,8] Because non-uniformities in the electric field might be of importance in atmospheric breakdown, a study of a high mode cavity was made. A

cubical cavity resonant in the TM_{230} mode was constructed and breakdown measurements in air, nitrogen, and oxygen were made. The results are shown in Figure 30. A mathematical analysis of the diffusion equation for this case was also carried out. The complete calculation and the details of the interpretation are given in Technical Note No. 1.[9] The results of the mathematical analysis and the experiment indicate that the electrons diffuse from the areas of high electric field to those of low electric field and produce an electron concentration profile which somewhat resembles what one would get for a uniform field and for the lowest diffusion mode. Figure 31 shows the electron profile across the two mode direction of the cubical cavity. This may be compared with the sinusoidal concentration profile which would exist for the lowest diffusion mode. The details of the calculation are contained in the Technical Note and will not be repeated here.

4. Theoretical Analysis of CW Data.

A phenomenological description of how microwave breakdown in gases takes place has been available for some years. When a high frequency electric field is applied across a gas, any electrons which happen to be in the field region are accelerated, collide with neutral atoms, are again accelerated, and in this process gain energy. As they gain energy from the electric field, which does not sweep them out of the region because it changes direction very rapidly, they lose energy in a number of different ways. First, there is some

energy loss because of the recoil from the neutral atoms, which are very much heavier than the electrons. Then, as they acquire energies of the order of a few volts, they can excite the atoms to more energetic states; and, finally, when they reach ionization energy they can, upon colliding with neutral atoms, ionize them. This process gives us two electrons where before we had one. The entire process takes place at a very rapid rate, and the numbers of electrons which are produced are very large.

At the same time, in addition to electron energy losses, there are particle losses, whereby some electrons disappear from the region in which the field is applied. Electrons may disappear from the discharge by diffusion, attachment, or, under some circumstances, recombination. Diffusion is simply the process of reaching the container walls by the random motions of the particles. Attachment is the process whereby electrons may be effectively removed from the discharge by becoming attached to a neutral particle; because of the extremely large mass difference between the atoms and the electrons, their accelerations thereafter in the microwave field are reduced so much that they are lost to the discharge. This is the process which takes place in oxygen and some other electro-negative gases. Recombination depends on the collision of an electron with a positive ion and is not important for the experiments reported here.

In actual fact, of course, the electrons have energies and velocities varying over very great ranges, and the proper description of the problem requires a statistical analysis. This kind of

analysis can be based on the Boltzmann transport equation, which is a differential equation from which can be determined, under some conditions, the electron velocity distribution function. If the electron velocity distribution function is known, we can then calculate, by standard kinetic theory formulation, ionization rates and loss rates for the electrons; combining these with the breakdown condition, which requires that the electron production equal or slightly exceed the electron loss rate, we can obtain a complete mathematical description of the problem.

This kind of calculation has been carried out only for the cases of certain atomic gases and hydrogen. The Boltzmann equation becomes unmanageably difficult unless certain approximations can be made in the function which describes the electron-neutral particle collision frequency. If the electron-neutral particle collision frequency is independent of electron energy, the Boltzmann equation can be very considerably simplified and, in fact, solved with a minimum of other approximations by introduction of the effective field discussed in Section 1. As noted in Section 1, it then becomes possible to describe breakdown fields by plotting E_e/Λ as a function of $p\Lambda$ and thereby representing the breakdown fields for a wide variety of pressures, container sizes, and frequencies by a single curve in two dimensions rather than a surface in three dimensions. Because of the economy of description thus afforded, many attempts have been made to describe the breakdown in air and in atmospheric gases in the same manner. Unfortunately, however, the collision

frequency of electrons with neutral particles in air, in oxygen, and in nitrogen departs very substantially from a constant. We have made attempts, as have others, to find an average collision frequency which, though not exactly correct, would present all the data in a single curve. Figure 32, which includes our data and some of that from Herlin and Brown, shows that this cannot readily be done for air. In those cases where the characteristic diffusion length is relatively small compared with the free-space wavelength of the electric field, the experimental data thus far obtained do come fairly close to a single line, and for some purposes this is a sufficiently accurate description. However, as will be noticed from the figure, for large Λ and small $p\Lambda$ there is a significant departure from this line. It should be pointed out that for Λ sufficiently large that $p\Lambda$ is above 10 cm - mm Hg, all curves for all frequencies and container sizes form a single straight line, giving a ratio of $(E_e\Lambda/p\Lambda)$ of approximately 30 volts per cm - mm Hg. If the product $p\lambda$ is large enough (greater than 100 cm - mm Hg) then E and E_e are approximately the same so that from this curve we can get, for these conditions, a value of the breakdown field and power, appropriate when microwave energy is radiated into very large volumes. However, since these are somewhat restricted conditions, we have devised an alternative representation which does not use the effective field except in an indirect way and, therefore, provides a more accurate description of the experimental data. This does not represent a theory in the same sense as the theoretical analyses which have been done for helium, hydrogen, neon,

and argon; but, at the same time, it does use some of the basic ideas of these theories and presents in an empirical manner a method for calculating breakdown fields for a very large variety of conditions. Also, as will be shown in a later section, it can be used for pulsed as well as cw processes.

As mentioned above, the two methods whereby electrons are lost to the discharge in air are diffusion and attachment. We represent by ν_a the attachment rate and by ν_i the ionization rate, and we may write the breakdown condition as follows:

$$\nu_i = \nu_a + (D/\Lambda^2). \tag{3}$$

The term D/Λ^2 is the rate at which electrons are lost by diffusion. If we knew the diffusion coefficient, D, under all conditions, we could find a direct value for the net ionization rate, $\nu_i - \nu_a$, from a set of experimental breakdown data.

The value of D has not been measured for conditions of high electric fields in air. A correct value of D will, of course, depend on the electric field, on the pressure, and on the nature of the electron velocity distribution function. A calculation of the product D multiplied by the pressure has been made for the cases of Maxwellian and Druyvesteyn distribution functions under certain assumptions as to the collision cross-sections. Subject to the approximations, which have been found to be reasonably good, we may

write out the diffusion coefficient in the following way:

$$Dp = 3.2 \times 10^5 \bar{u}, \tag{4}$$

where $\bar{u}$ is the average electron energy.[10] Values of the average electron energy, $\bar{u}$, have not been measured for high electric fields. However, Crompton, Huxley, and Sutton have made measurements of the average electron energy in air for values of E/p up to about twenty-five (volts per cm - mm Hg).[11] These data, combined with Equation (4), give us values of Dp as a function of E/p. This is plotted in Figure 33. We have plotted the results in terms of E_e/p instead of E/p, because it seems reasonable that the average energy will depend in some way on the E_e rather than E. At high frequencies, of course, the energy gained by the electrons is reduced by the E_e/E factor. In calculating E_e for this purpose we have used the value $\nu_c = 5.3 \times 10^9 p$. We extrapolate the straight line portion of this curve to give an empirical estimate of the product Dp. This results in the equation

$$Dp = \left[29 + 0.9\ (E_e/p)\right] 10^4 \qquad (cm^2 - mm\ Hg/s) \tag{5}$$

where the units of E_e are volts per cm and of p are mm of Hg.

As pointed out above, at breakdown $\nu_i - \nu_a = D/\Lambda^2$. Using our value of D from Equation (5) we can calculate a series of curves showing the net ionization, $\nu_i - \nu_a$, as a function of $p\lambda$ for different values of $E\lambda$. We make this calculation by taking the

breakdown data and manipulating them in the following manner. For a given value of breakdown field at a particular pressure as determined from the breakdown curves, we calculate Dp from Equation (5), multiply it by $(\lambda/\Lambda)^2$, and divide by $p\lambda$. This then gives the product $D\lambda/\Lambda^2$, which at breakdown is equal to $\nu\lambda$. Proceeding in this manner we can construct a series of curves which are shown in Figure 34.

We can write $D\lambda/\Lambda^2$ alternatively in a slightly different manner by taking the value which we had for Dp from Equation (5), multiplying by $(\lambda/\Lambda)^2$, and dividing by $p\lambda$. This results in the following equation:

$$D\lambda/\Lambda^2 = 10^4(\lambda/\Lambda)^2 S, \tag{6}$$

where S is given by

$$S = 1/p\lambda \left[29 + \frac{0.9\ E\lambda}{\sqrt{(p\lambda)^2 + (35.6)^2}} \right] . \tag{7}$$

The term S is plotted in Figure 35 for a number of different values of $E\lambda$, as a function of $p\lambda$.

If we now were to plot this curve on transparent graph paper, we could see that by multiplying the line where S = 1 by the factor $10^4(\lambda/\Lambda)^2$ we would have the values of $D\lambda/\Lambda^2$ plotted as a function of $p\lambda$. We can then superpose this on our previous graph and where the lines of the same $E\lambda$ intersect on the two graphs we have the breakdown condition. It can thus be readily seen that by combining

these two curves we can extract breakdown data for a great variety of conditions. For example, if we have a known frequency and a known container size, we can immediately determine at what vertical height on Graph 34 we set Graph 35; and immediately we have the values of $E\lambda$ and $p\lambda$ for breakdown conditions. It is then a simple matter to construct an E-p breakdown curve.

The data from which these graphs were compiled include all the cw data shown in Figures 4 through 23 at frequencies of 1, 9.4, and 24 kMc/s, as well as the data of Rose and Brown.[4]

5. Theoretical Analysis of Pulsed Data.

One considerable advantage of the method of presentation of the breakdown curves employed in the previous section is that Figure 34 can be readily adapted to calculations of pulsed breakdown. When an electric field is applied to a gas for a very short period of time, the process which goes on is, of course, essentially the same as that which happens when we are considering cw breakdown. However, there is a short period of time when the pulse is initially applied which is required for the electron concentration to build up. During this period of time the electron concentration is given as a function of time by the equation

$$n = n_o e^{\nu t}. \tag{8}$$

In this equation the ν means the net ionization rate; in other words,

in the case of air ν is equal to $\nu_i - \nu_a - (D/\Lambda^2)$. It is therefore a measure of the excess of the production rate of electrons over the loss rate.

We may say that breakdown takes place for pulsed conditions if the electron concentration reaches the plasma concentration value by the end of a given pulse. We will assume for the purposes of this calculation that the time between pulses is sufficiently long so that there is no large number of electrons left over from one pulse to influence the next. We may, therefore, set as a criterion for breakdown the condition that

$$n_p = n_o e^{\nu \tau}, \tag{9}$$

where n_p is the plasma concentration, which is equal to $10^{13}/\lambda^2$ (λ is the wavelength in centimeters), if the concentration is measured in number of particles per cubic centimeter, and where τ is the pulse length.

The initial concentration of electrons is not accurately known; however, because of the exponential nature of the phenomenon, the results which one obtains by varying the initial electron concentration between $1/cm^3$ and $1000/cm^3$ are not very different. In the experiments which were carried on in this laboratory we used a 5 millicurie radioactive cobalt source, which produced in most of the cavities an electron concentration of approximately one hundred electrons per cc. In the absence of an electron from a

radioactive source, the breakdown fields are considerably larger because it may very well happen that during the relatively small fraction of time that the electric field is on, natural cosmic radiation will not produce any electron within the region where the electric field is large.

In applying the results of these experiments to breakdown in the atmosphere, one must be careful to realize that breakdown will not take place at all if there are no electrons to provide the initial ionization within the region in which the electric field is applied. Therefore, the pulsed breakdown conditions which we derive are in the nature of a lower limit of the field or power which is required to produce breakdown.

We can then use Graph 34 directly to calculate breakdown fields in the following manner. Given the cavity size, which gives us Λ, we first calculate the value of D/Λ^2, which we can do by estimating the breakdown field to give us the value of D from Equation (5). We use Equation (9) and find out what value of $\nu\tau$ is required to produce plasma concentration for the wavelength under consideration and then, knowing the pulse lengths we are dealing with, we can calculate the ν. The ν of Figure 34 is equal to $\nu - \nu_a$, but knowing the net ν and the D/Λ^2 we can calculate directly ν and $\nu\lambda$. Then, knowing $p\lambda$, we can read off directly the field $E\lambda$. In Figures 18 and 19 are shown the results of calculations by this procedure for pulsed breakdown in a cavity at X-band with pulses of various durations and with a repetition rate of 1000 per second. The dashed

lines are the calculations predicted from this curve; the points are the experimental measurements. Similar calculations and experiments for L-band are shown in Figure 9. Except at the very short pulse lengths where the pulse length is not well known, there is remarkable agreement between the calculations and the measured points.

B. SCATTERING AND ATTACHMENT CROSS-SECTIONS.

It is clear from the discussion in Section A that two of the most important parameters in breakdown analysis of air are the electron-molecule collision scattering cross-sections and the attachment frequency. These parameters enter in a complicated way into the processes which determine breakdown. When the experimental program was set up neither of these parameters was very well known, particularly at the lower energies; and it was decided that a Ramsaeur-type experiment, which would enable us to determine unequivocally the collision frequencies and the attachment frequencies as a function of electron energy, would be a most valuable aid in understanding breakdown processes.

There have recently been a number of studies of different types of attachment in oxygen and in air, but there are still a number of unanswered problems. With regard to the collision cross-sections, or collision frequency, there has been relatively little work done since the late twenties and early thirties, and a good deal of that work is not accurate at the very low electron energies.

An experiment was devised to measure both scattering and attachment cross-sections. The many components of the exceedingly complex apparatus were designed and tested individually and are now being assembled. The experiment is perhaps described best in terms of a diagram (Figure 36) which is a schematic of the experimental apparatus. Electrons from a unipotential cathode will be selected as to energy by a uniform magnetic field and three slits arranged nearly along the arc of circle, 90° apart. From the last slit a monoenergetic beam of electrons will lead into the interaction region and will continue to curve in the magnetic fields. In this region, electrons still in the beam, neither scattered nor attached, will be collected on an electrode which can be moved along the beam. Ions formed by attachment will be collected perpendicular to the electron beam. In principle, from the measurements of ion and electron currents as a function of the length of the interaction region, both the scattering and the attachment cross-sections can be determined.

High speed pumps will be used to reduce the gas pressure in the energy selection region relative to that in the interaction region in order to minimize attenuation of the beam before it can be used. The major difficulties of this experiment are due to the very low electron energies required. As the energy is decreased, it becomes increasingly difficult to obtain useable numbers of electrons, and their energies and trajectories are more seriously altered by slight fields, contacts potentials, and the presence of charges.

The details of the calculations relative to the feasibility of the experiment are contained in the Final Report of May, 1961,[2] and will not be repeated here. During the course of the work the emphasis and the primary considerations have shifted from that of attachment to scattering. Because of the growing interest in the low energy collision cross-sections and the lack of any experimental results to go along with a good deal of theoretical work which is being done here and elsewhere, the first measurements which will be done with this apparatus will be those of scattering in atmospheric gases. The scattering experiments are somewhat easier to do and there is no doubt that we can get to very much lower beam energies than has been the case previously. The following paragraphs will indicate the considerable difficulties that have been involved in providing cathodes suitable for work with oxygen. While this work on cathodes is proceeding, we will continue to work on the scattering experiments since they do not require the cathode which will be suitable for the attachment measurements in oxygen.

During the period of this report experimental testing was performed to fix dimensions of the copper gasket seals to meet special requirements of this experiment. Also, with the completed vacuum system, some experimentation was done with differential pumping to determine slit sizes in the apparatus. With this information the dimensions of the apparatus were determined and design and construction details worked out, and detailed drawings were made. All of the parts

except for the cathode have been completed and most of the assembly has been accomplished. Because of the considerable effort involved in developing suitable cathodes, it perhaps warrants some detailed reporting.

Requirements, and the original design for the cathode, were discussed in the above-mentioned Final Report. Tests of that design showed that the cathode ribbon made very poor thermal contact with the heater box, and that after the heaters had burned out there was a heavy dark deposit on the ceramic where the front array of heaters had been. This appeared to be evaporated tungsten. It was thought that it had caused shorting between the heater elements and had occurred because of voids where the ceramic powder did not fill in under the form on which the heater wires were mounted.

The design was then changed to have the cathode ribbon spring loaded against the heater box and the heater elements supported only from their lead-ins so that the ceramic powder could be filled in around them without voids. Considerable difficulty was encountered with heaters breaking in assembly, but techniques were developed to overcome this. When the design was finally tested, the thermal contact between cathode ribbon and heater box was still not very good; but a more serious difficulty was encountered in that at temperature above about 1700° C the tungsten and Al_2O_3 combine to form an alloy which conducts electricity and shorts out the heaters. This limitation on heater temperature, together with the thermal insulation of the ceramic and the poor thermal contact of the ribbon, made it

impossible for that design to get the cathode ribbon up to required temperatures.

Two quite different methods of indirectly heating a thoria-coated cathode to 1350° C have been thought of. One, which depends mainly on raising the limit of heater temperature, is to mount an array of iridium heaters so that they are surrounded on three sides by ceramic thermal insulation and on the fourth by the thoria-coated iridium cathode. Iridium is quite rigid, melts at 2454° C, and does not oxidize; so the heaters with no contact to the ceramic could run quite hot. Heat transfer would be mainly by radiation with some assist from gas and electron conduction. Tests of this are now being made. Another method, which aims chiefly at improved heat transfer over previous designs with some increase in heater temperature, is to put only about .005" of sintered Al_2O_3 insulation on the heaters and then sinter platinum powder onto the ceramic coating to get good thermal contact. The sintered platinum serves as the cathode base with the thoria coated directly onto it. The thin ceramic coatings would not give protection from the atmosphere, so the heaters must not be subject to oxidation and should also be of a material which will not alloy with the ceramic. Iridium again appears to be the best material but some work has been done with this design using 20 percent Rh-80 percent Pt heaters. These have not yet achieved temperatures sufficient for thoria coatings, although they have given some emission; but they have been operated for some periods of time at temperatures from 1100 to 1200° C, which is more than enough to activate conventional oxide coatings. It thus

appears that we can now make cathodes which, by using conventional coatings, can satisfy all of the requirements of this experiment except the ability to work in oxygen.

We are now continuing further cathode development as a side experiment of secondary importance and proceeding with the main experiment using conventional oxide coatings. The first work will be retarding potential measurements to determine energy spread of the beam and the lower limit of attainable electron energy in vacuum. This must be done where the beam first leaves the last slit and again some distance from it to be sure the electrons follow proper trajectories. Some of this will then have to be repeated with gas flow in the apparatus to learn the limitations this may introduce. When this has been done, the apparatus will be ready to use for measurement of scattering cross-sections in gases other than oxygen. Work with oxygen can then be done when a successful thoria-coated cathode has been developed.

C. CONCLUSIONS AND RECOMMENDATIONS.

The analyses given in Section A represent not a theoretical derivation of all breakdown conditions based on the molecular processes, but rather a correlation of all the data which have thus far been obtained, in such a way as to enable reasonable interpolations and extrapolations to be made. The validity of the procedure is demonstrated by the agreement which is found between calculations made on the basis of these charts and actual experiment. Although we have

not yet a theoretical analysis of the breakdown problem in air based on a proper solution of Boltzmann's equation, it appears that the information that we now have is sufficiently accurate to make all necessary predictions. The present data and the method of interpreting them provide us with sufficient information to make calculations under those conditions which were envisaged when the experimental program was initially undertaken. It is not thought likely that further experimental data within the pressure ranges of atmospheric to that existing at 100 km and the frequency range from 100 Mc/s to 100 kMc/s would lead to conclusions any different from those contained in this report.

REFERENCES

1. A. D. MacDonald, "Electrical Breakdown in the Atmosphere," Scientific Report No. 1, Contract AF 30(602)-2261, Microwave Physics Laboratory, General Telephone and Electronics Laboratories, Inc., 8 December 1960 (RADC-TN-61-16).

2. A. D. MacDonald, H. W. Bandel, D. U. Gaskell, H. N. Gitterman, "Electrical Breakdown in the Atmosphere," Final Report, Contract AF 30(602)-2261, Microwave Physics Laboratory, 12 May 1961 (RADC-TR-61-135).

3. M. A. Herlin and S. C. Brown, Phys. Rev. 74, 291 (1948).

4. D. J. Rose and S. C. Brown, J. Appl. Phys. 28, 561 (1957).

5. L. Gould and L. W. Roberts, J. Appl. Phys. 27, 1162 (1956).

6. A. D. MacDonald and S. C. Brown, Phys. Rev. 75, 411 (1949); Phys. Rev. 76, 1634 (1949).

7. M. A. Herlin and S. C. Brown, Phys. Rev. 74, 1650 (1948).

8. A. D. MacDonald and S. C. Brown, Can. J. Res. A28, 168 (1950).

9. A. D. MacDonald, "Electron Diffusion in a Multimode Cavity," Technical Note No. 1, Contract AF 30(602)-2501, Microwave Physics Laboratory, 15 January 1962 (RADC-TDR-62-67).

10. A. D. MacDonald, Proc. IRE 48, 436 (1959).

11. R. W. Crompton, L. G. H. Huxley, D. J. Sutton, Proc. Roy. Soc. London A218, 507 (1953).

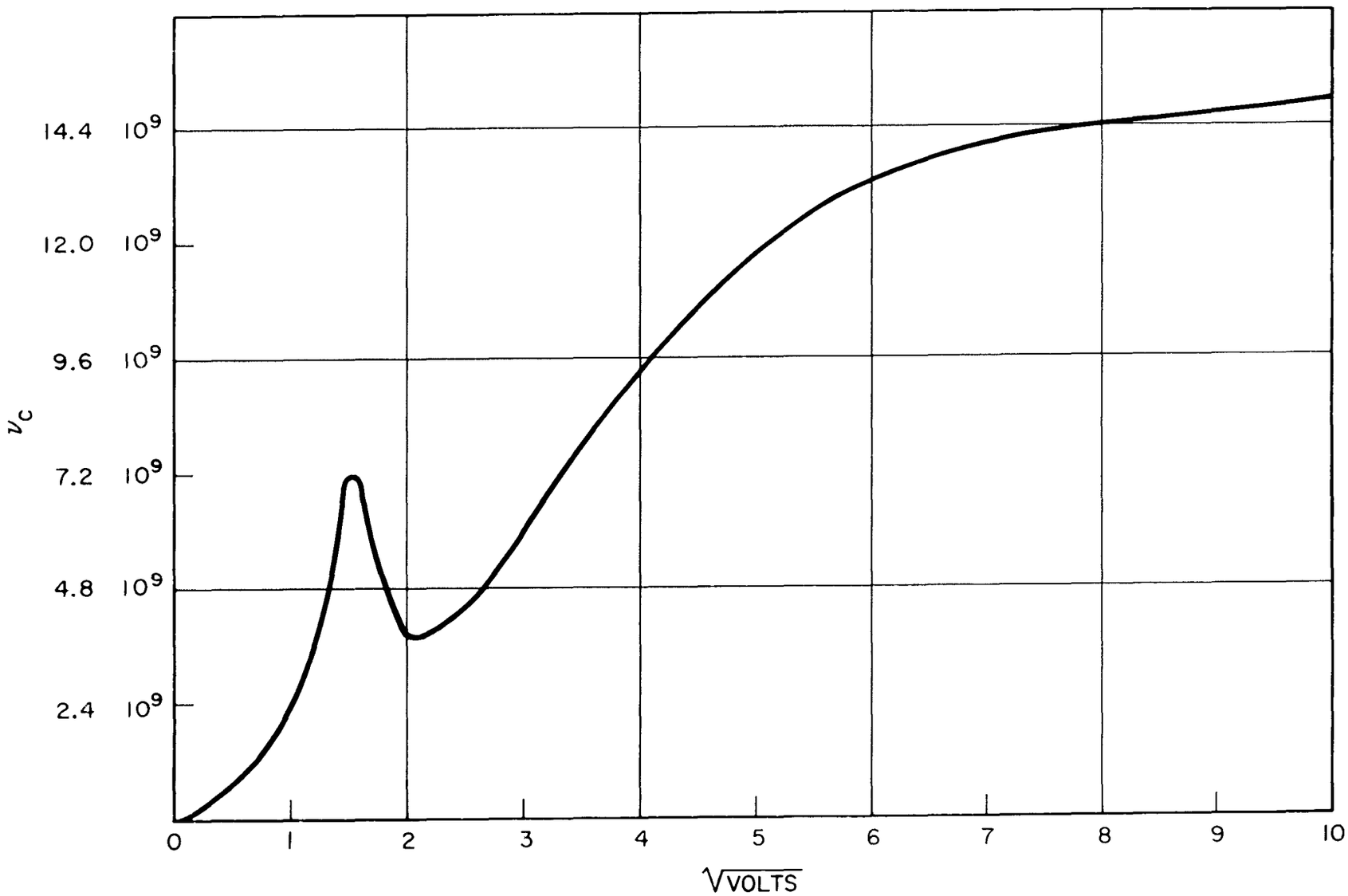

FIGURE 1

Collision Frequency for Electrons in Air

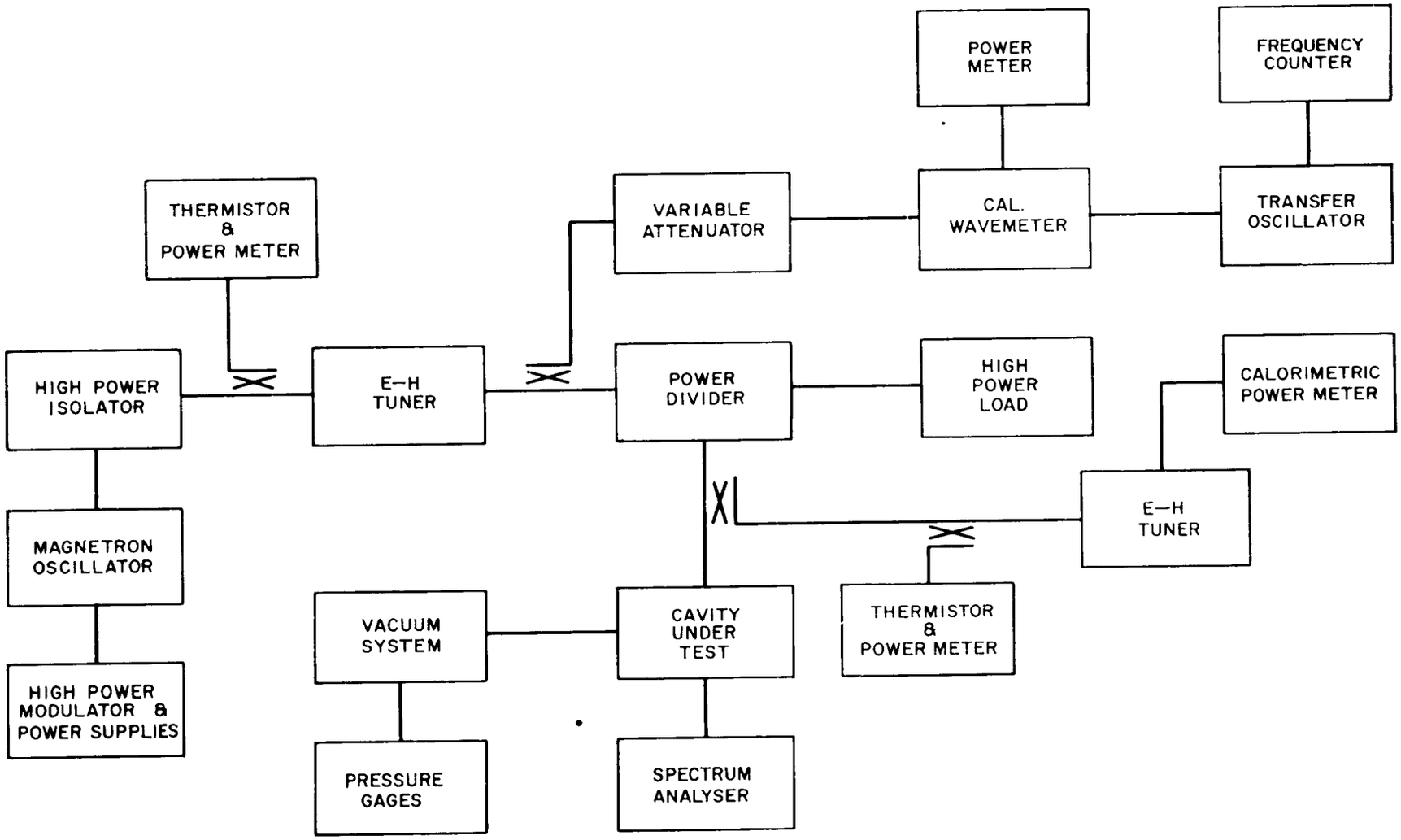

FIGURE 2

Block Diagram of Microwave Equipment for Breakdown Measurements

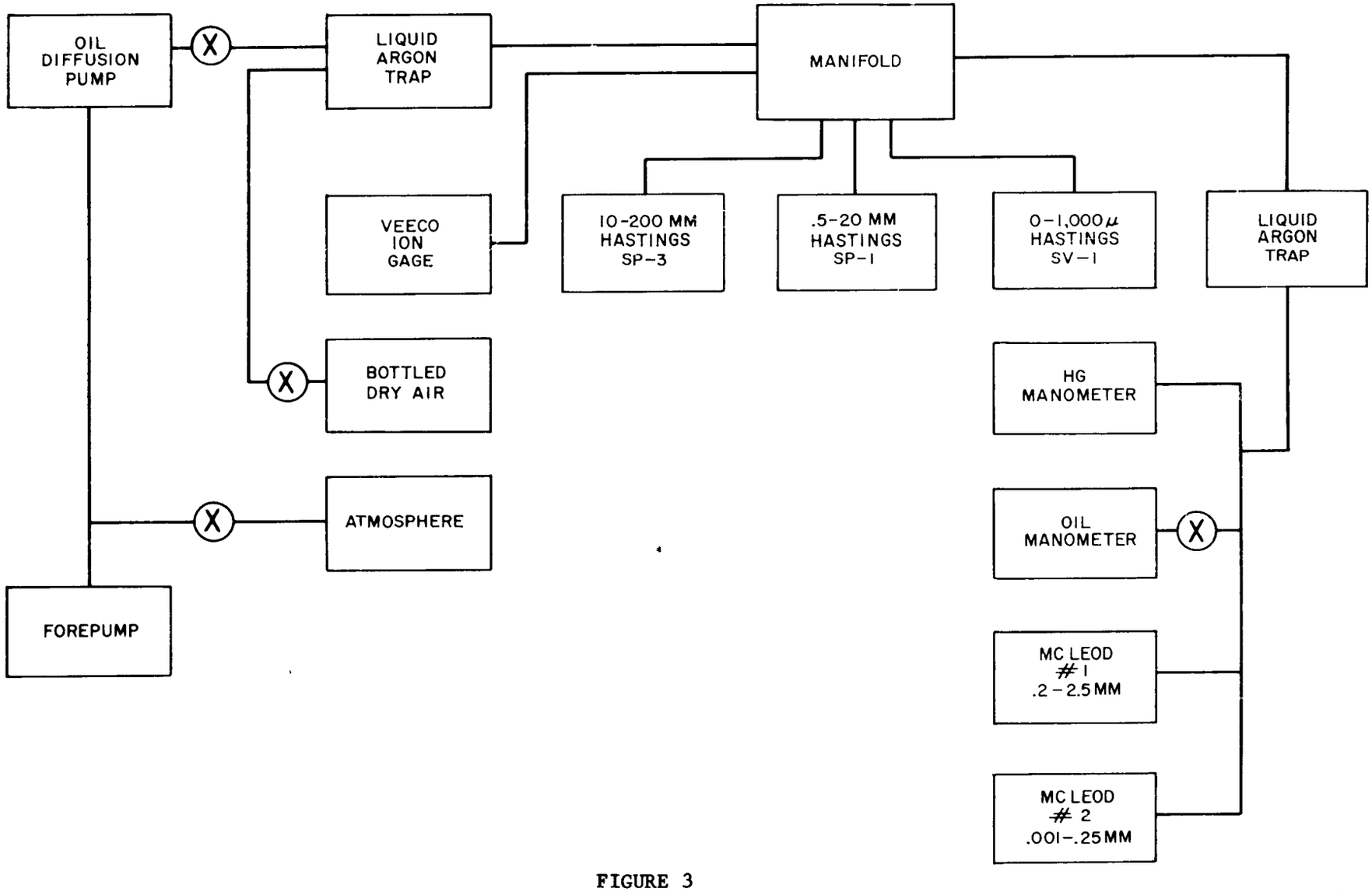

FIGURE 3

Typical Vacuum System (Oil Manometer Was Replaced with a Third McLeod Gauge for Later Measurements)

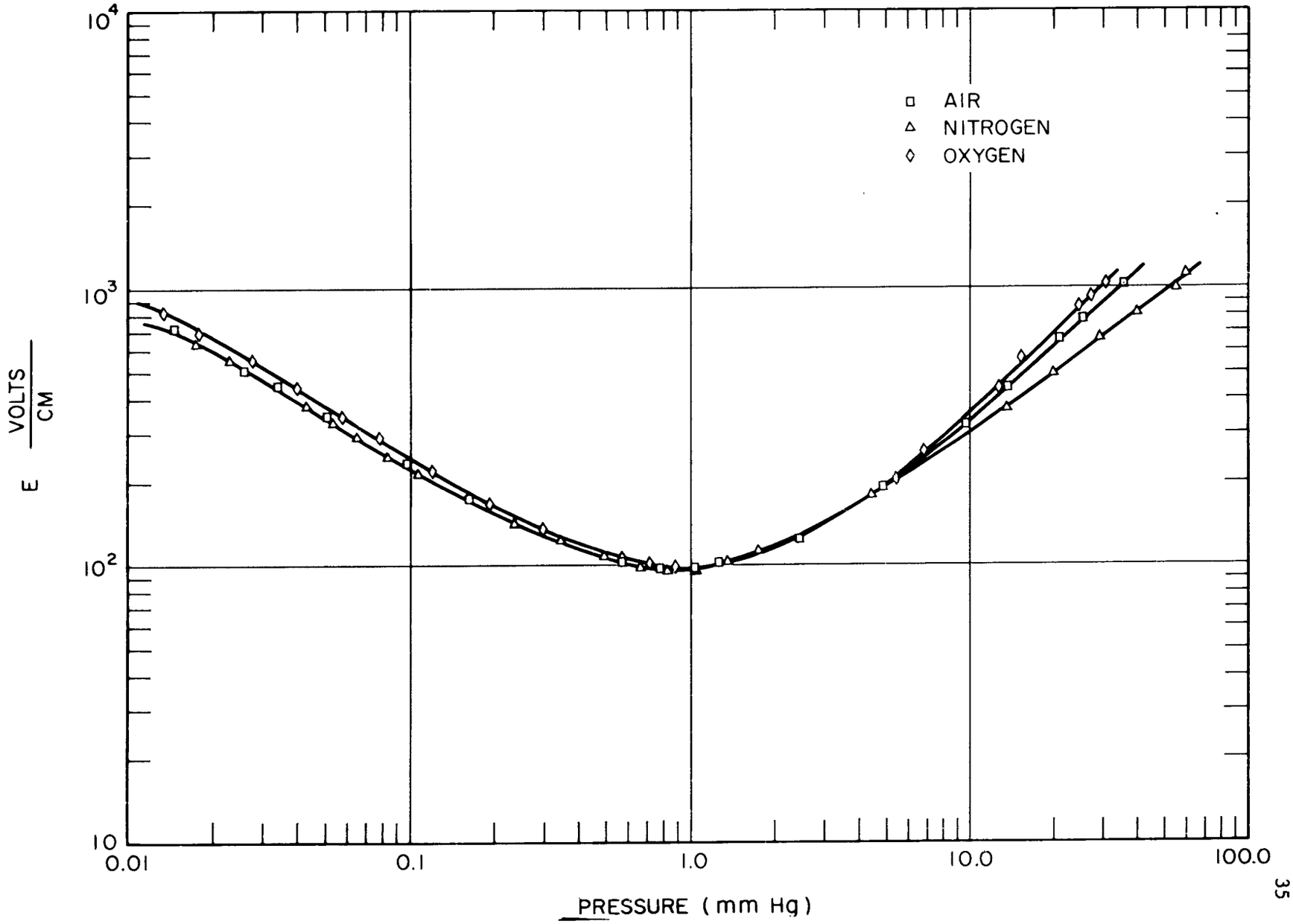

FIGURE 4

CW Breakdown in Air, Oxygen, and Nitrogen
(λ = 0.631 cm; f = 992 Mc/s)

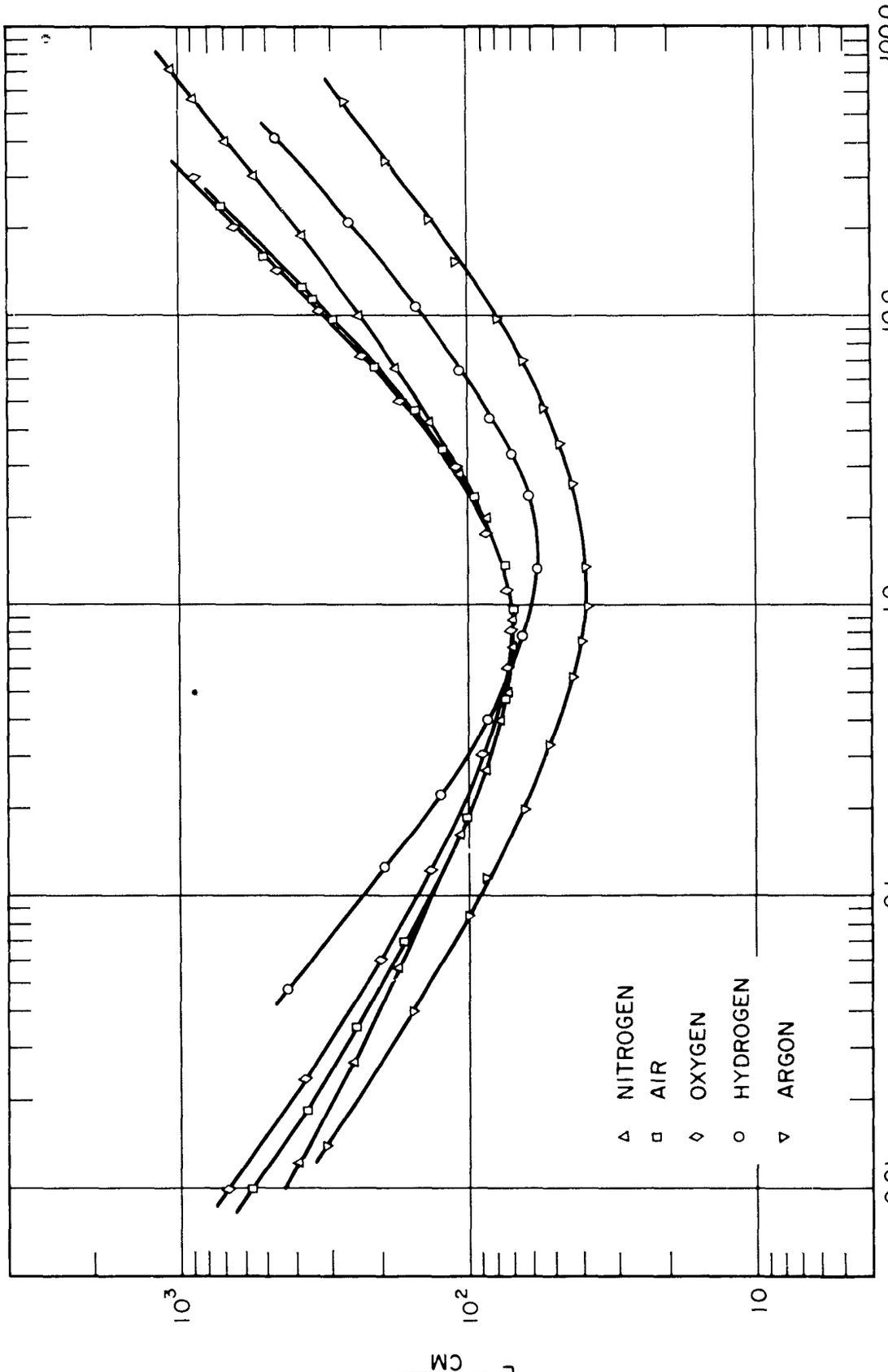

FIGURE 5

CW Breakdown in Nitrogen, Oxygen, Air, Hydrogen, and Argon (Λ = 1.51 cm; f = 994 Mc/s)

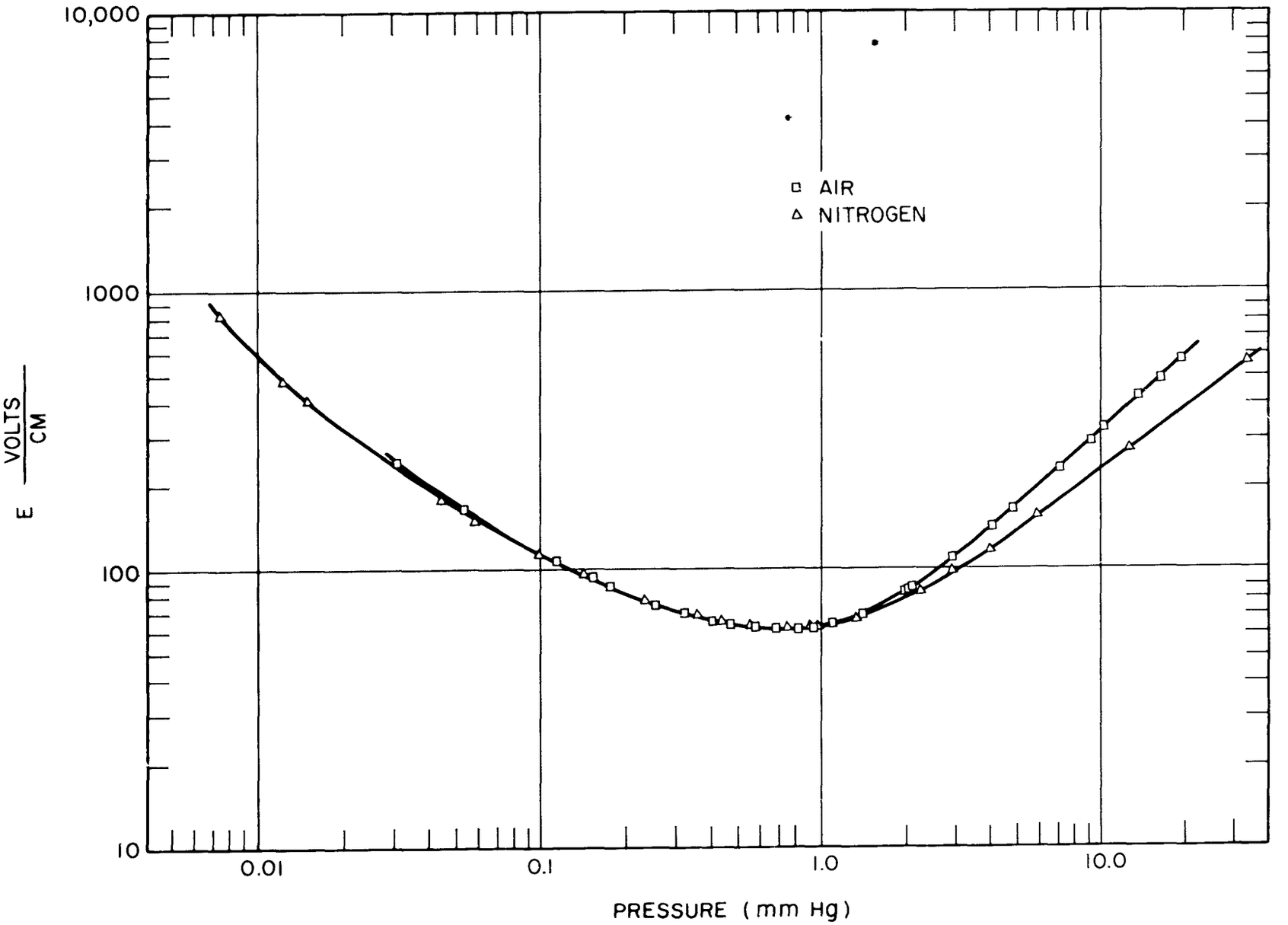

FIGURE 6

CW Breakdown in Air and Nitrogen
(λ = 2.65 cm; f = 994 Mc/s)

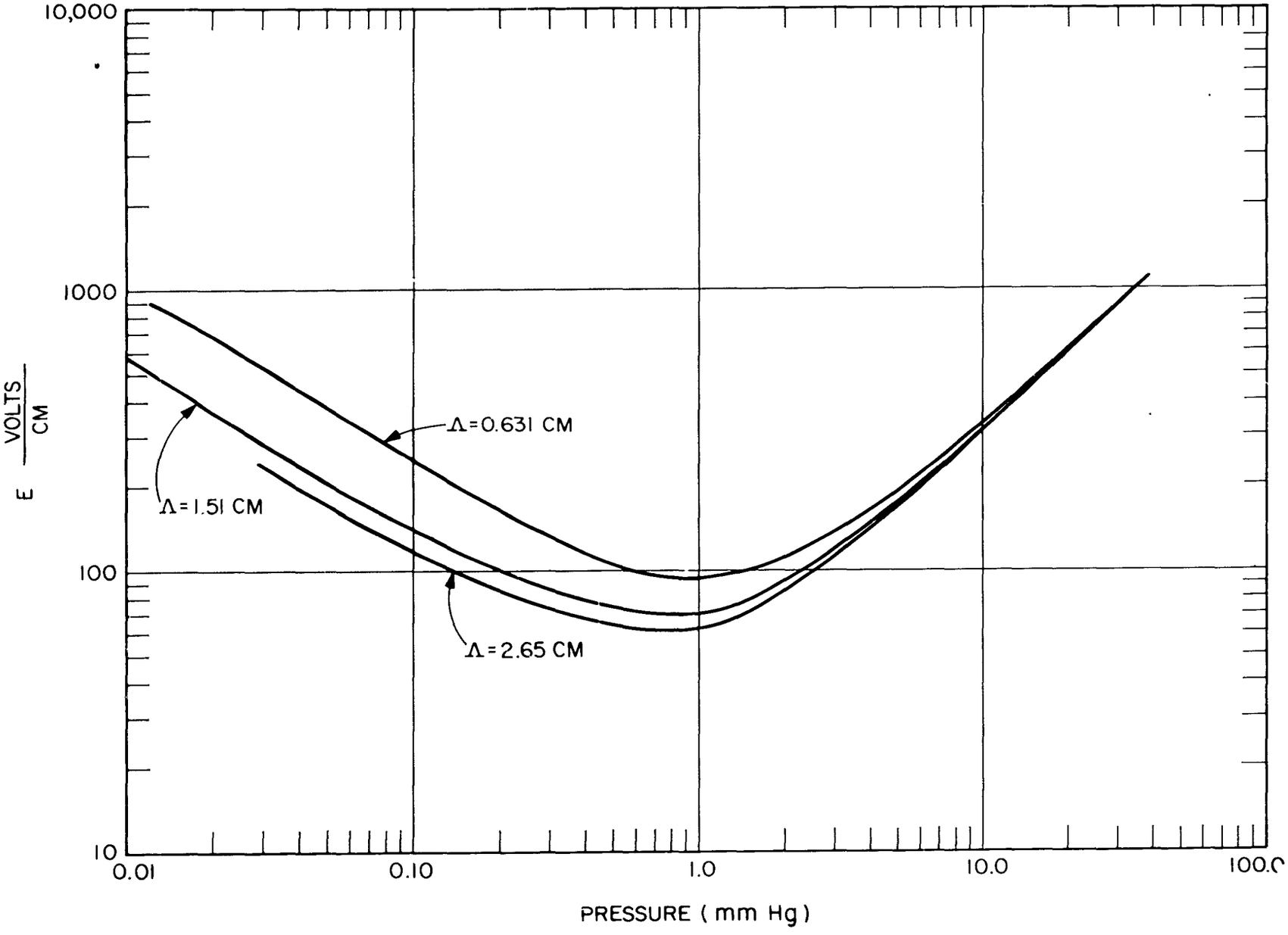

FIGURE 7

CW Breakdown in Air for Three L-Band Cavities

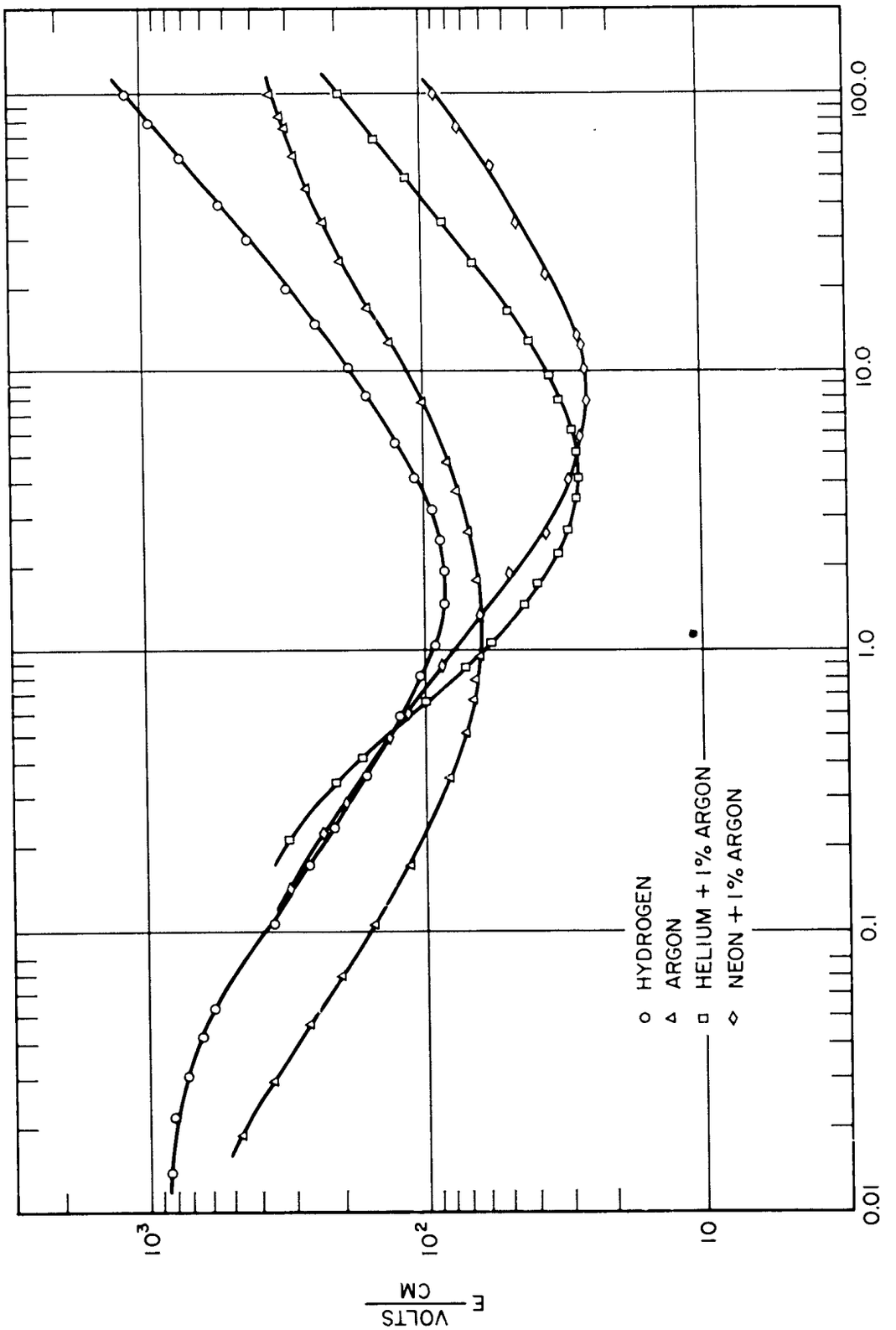

FIGURE 8

CW Breakdown in Hydrogen, Argon, Helium + 1 Percent Argon, and Neon + 1 Percent Argon (λ = 0.631 cm; f = 992 Mc/s)

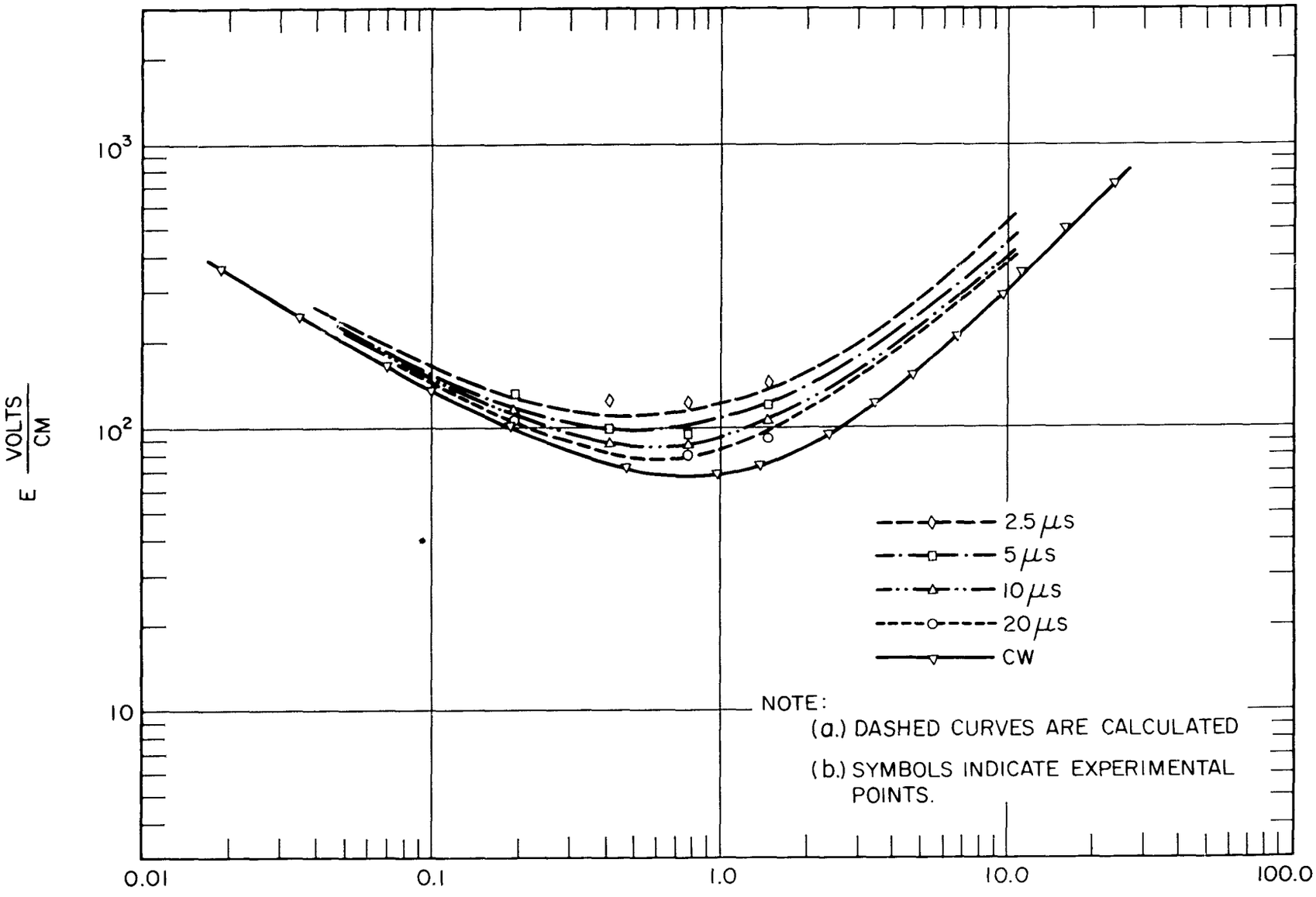

FIGURE 9

CW and Pulsed Breakdown in Air
(λ = 1.51 cm; f = 994 Mc/s)

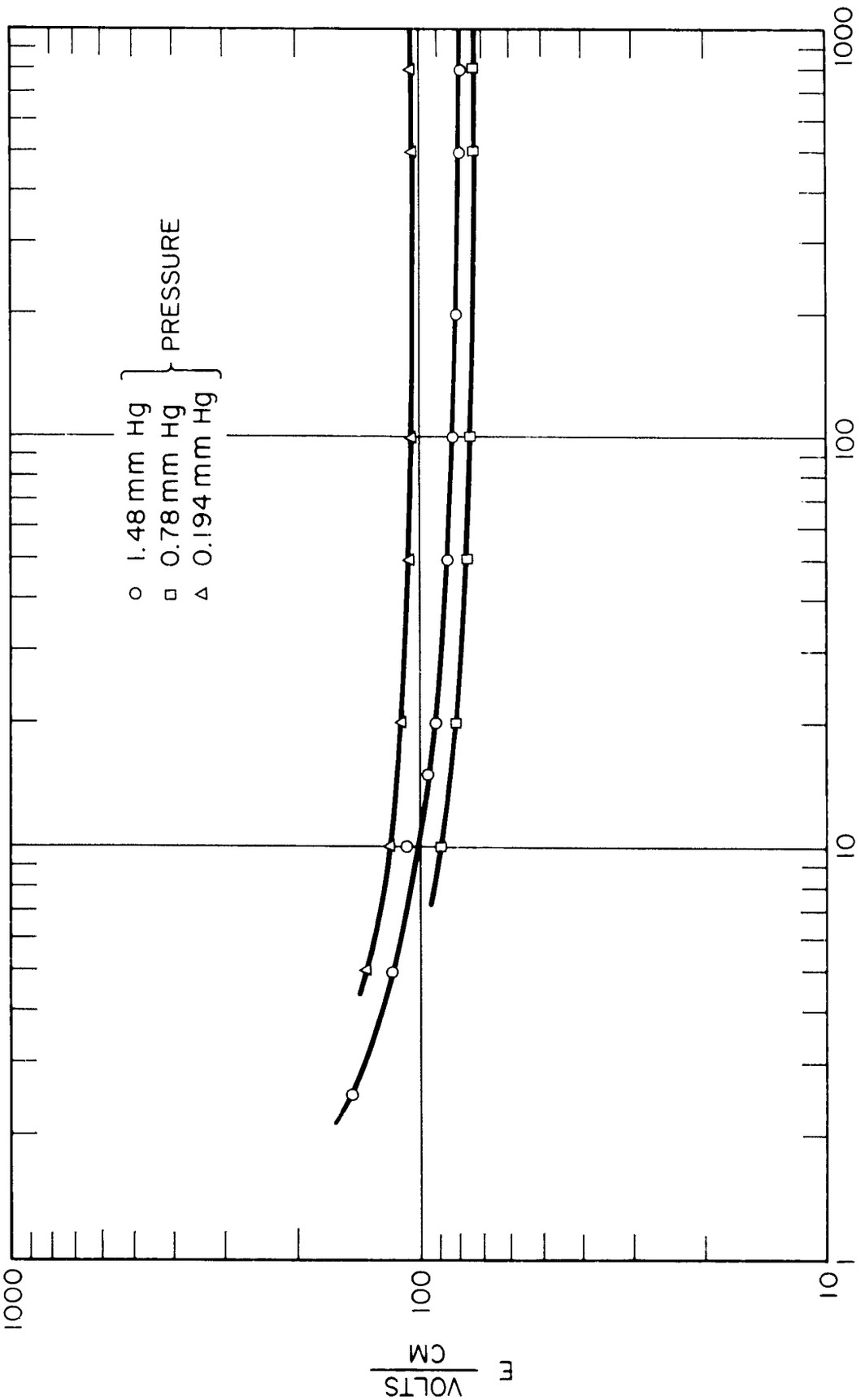

FIGURE 10

Pulsed Breakdown in Air for a rulse Repetition Rate of 1 kc
(Λ = 1.51 cm; f = 994 Mc/s)

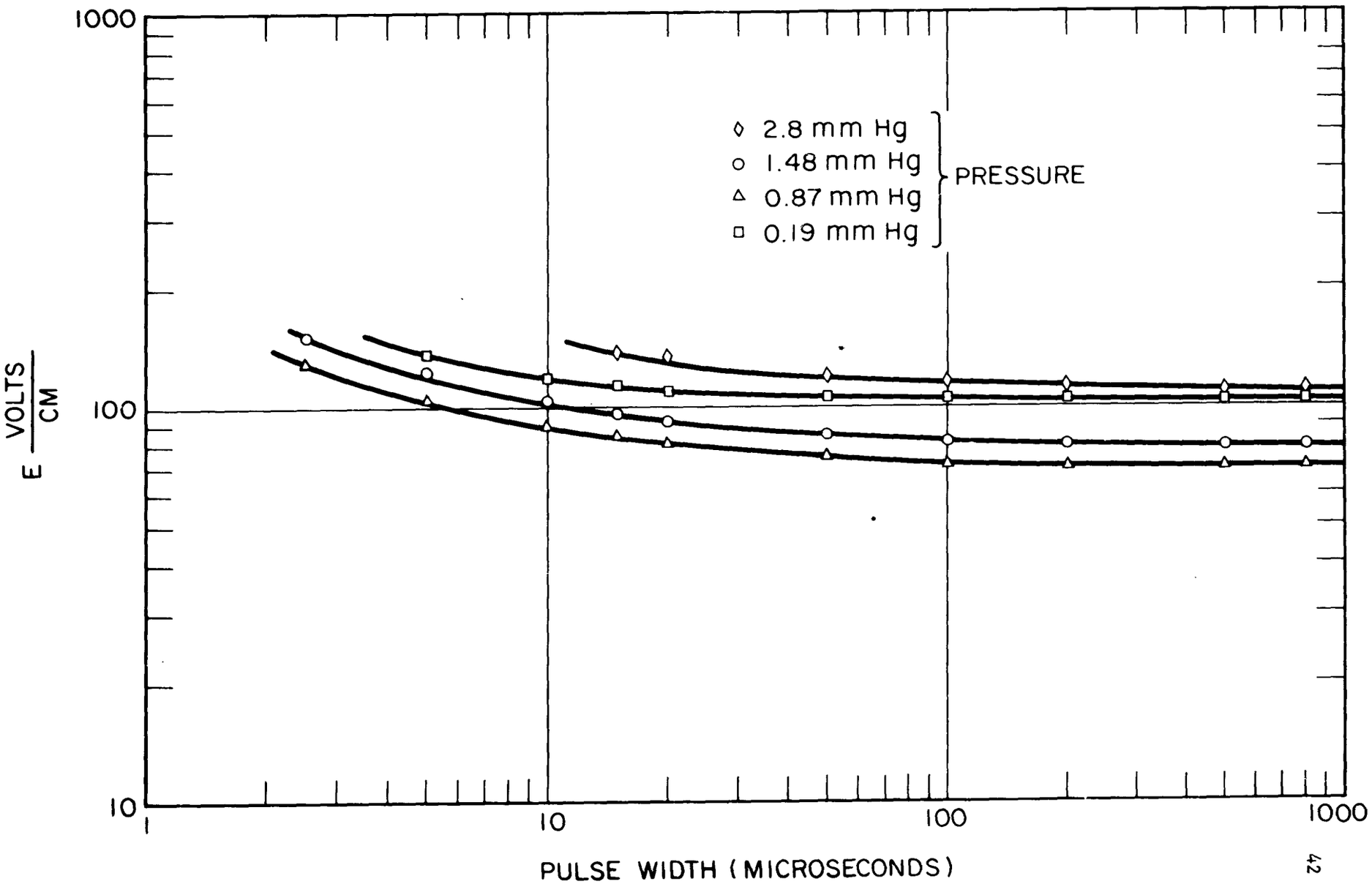

FIGURE 11

Pulsed Breakdown in Nitrogen for a Pulse Repetition Rate of 1 kc
(λ = 1.51 cm; f = 994 Mc/s)

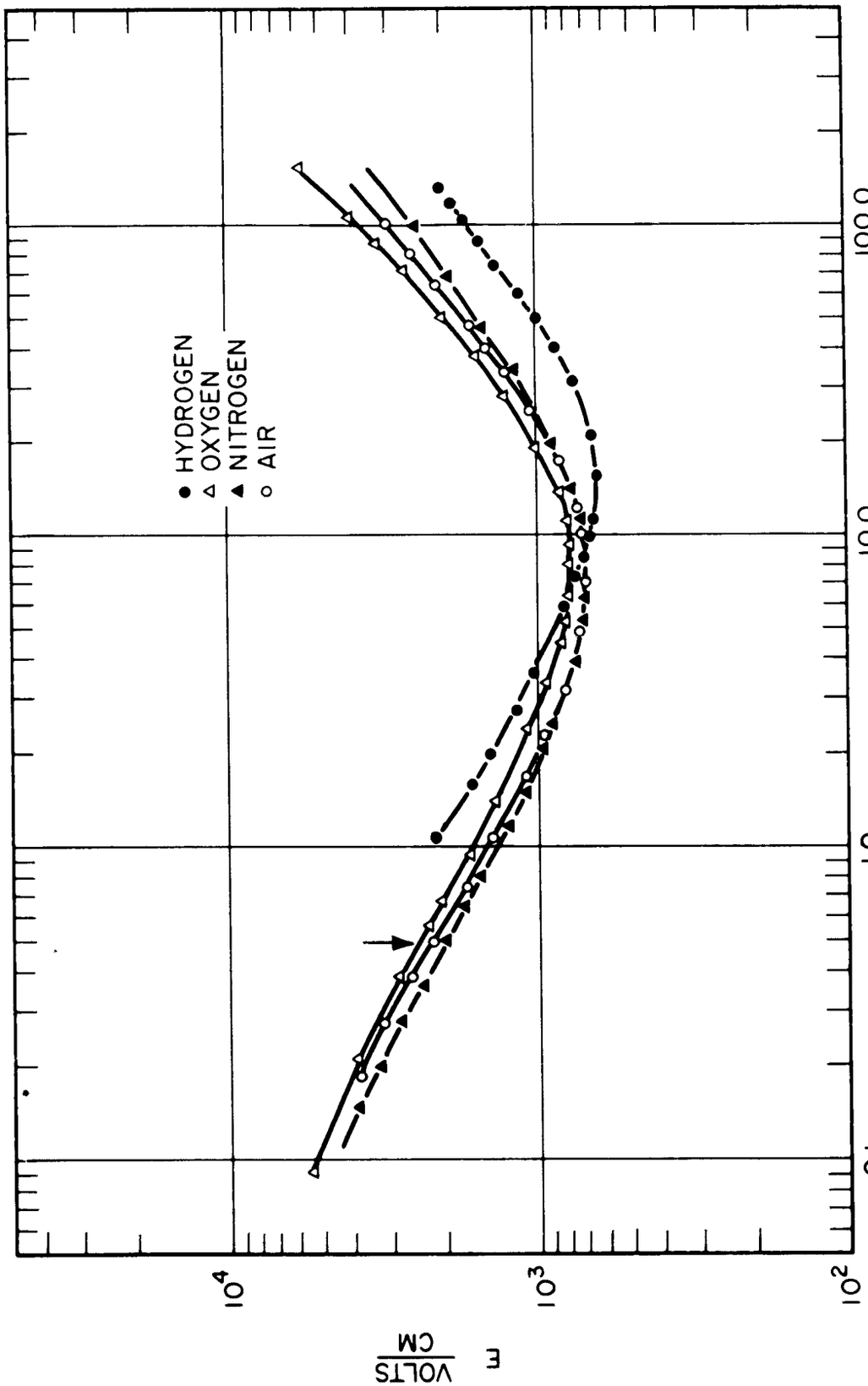

FIGURE 12

CW Breakdown Fields for Air, Nitrogen, Oxygen, and Hydrogen
(λ = 0.103 cm; f = 9.4 kMc/s)

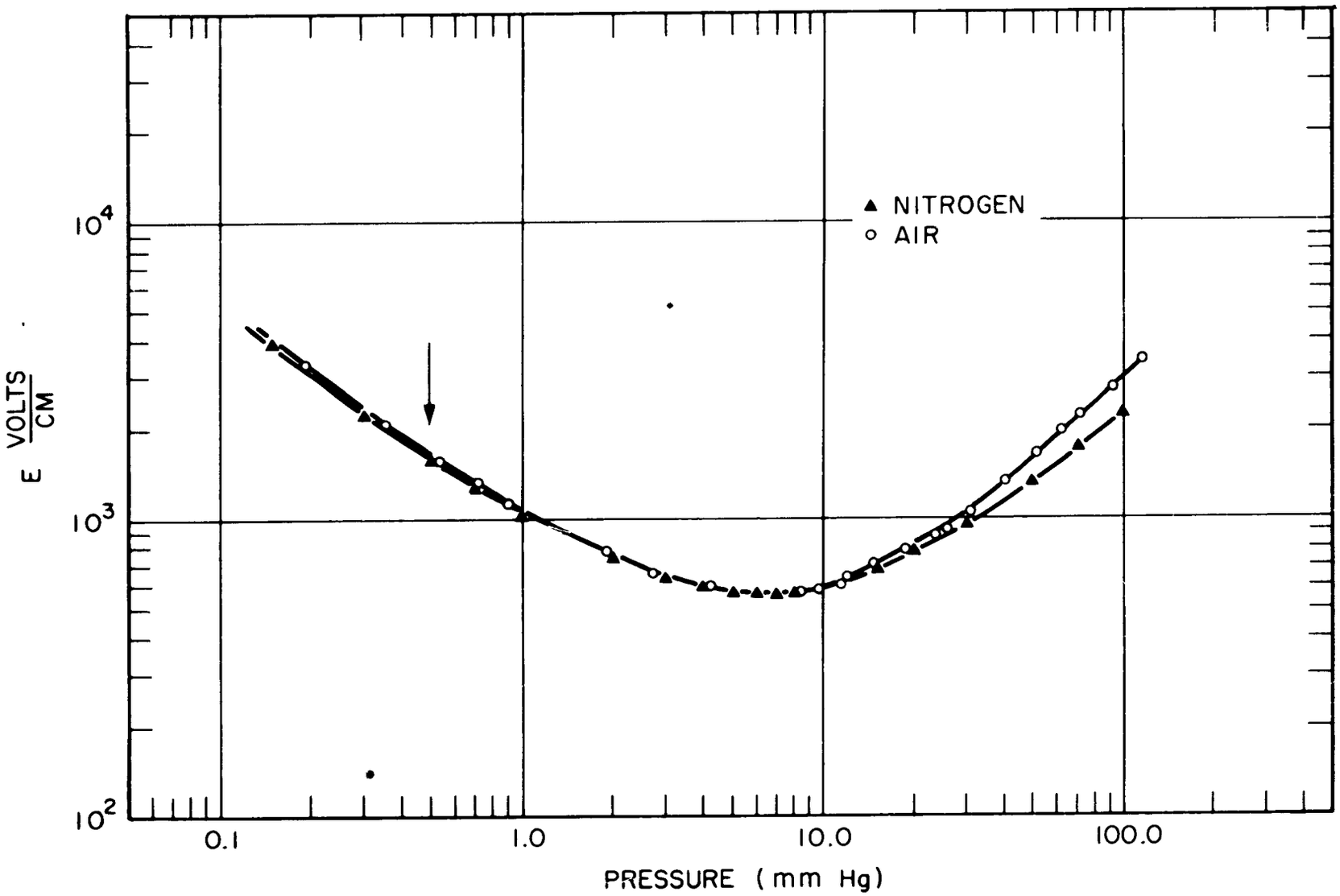

FIGURE 13

CW Breakdown Fields for Air and Nitrogen
(λ = 0.22 cm; f = 9.4 kMc/s)

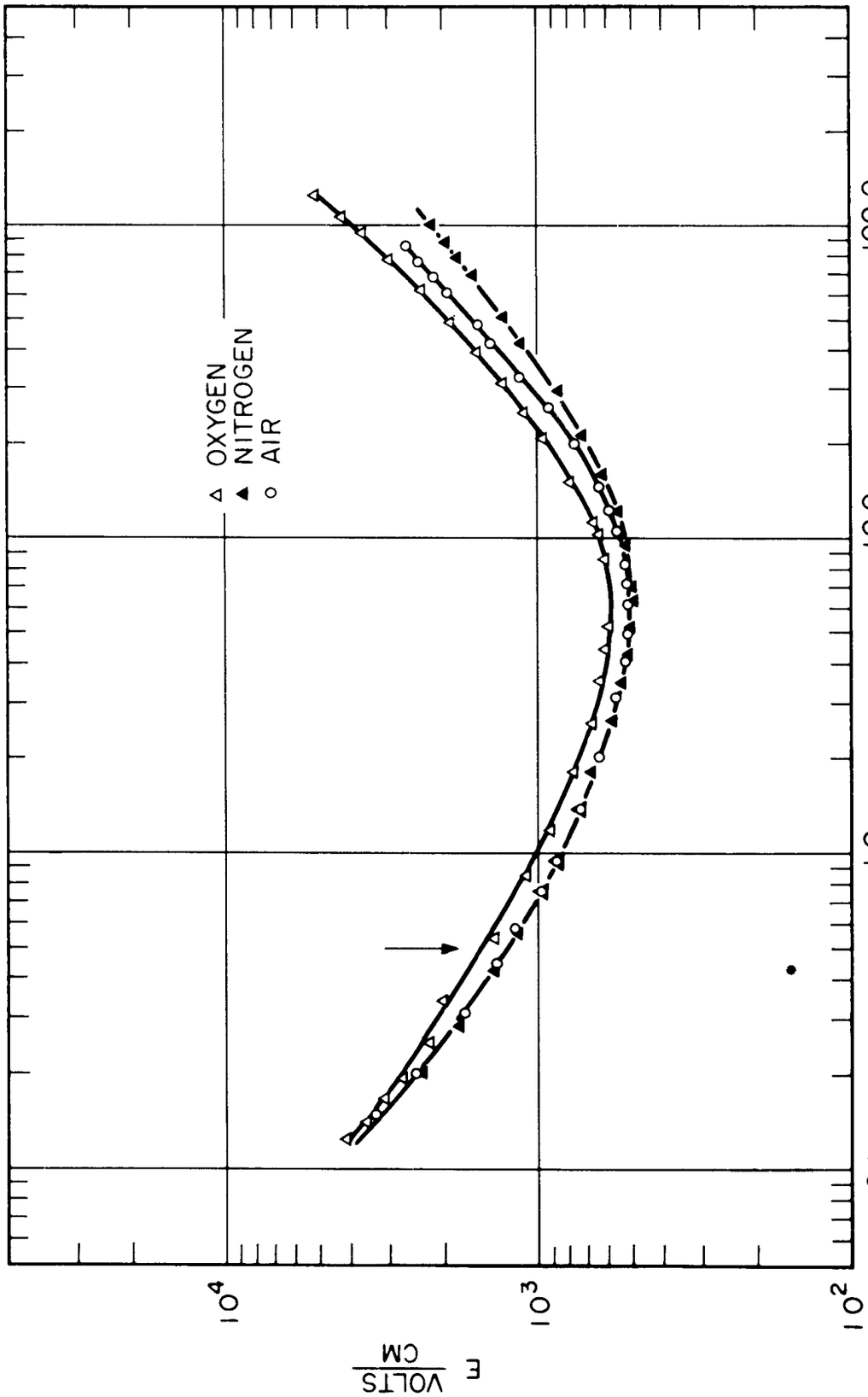

FIGURE 14

CW Breakdown Fields for Air, Oxygen, and Nitrogen
(λ = 0.40 cm; f = 9.4 kMc/s)

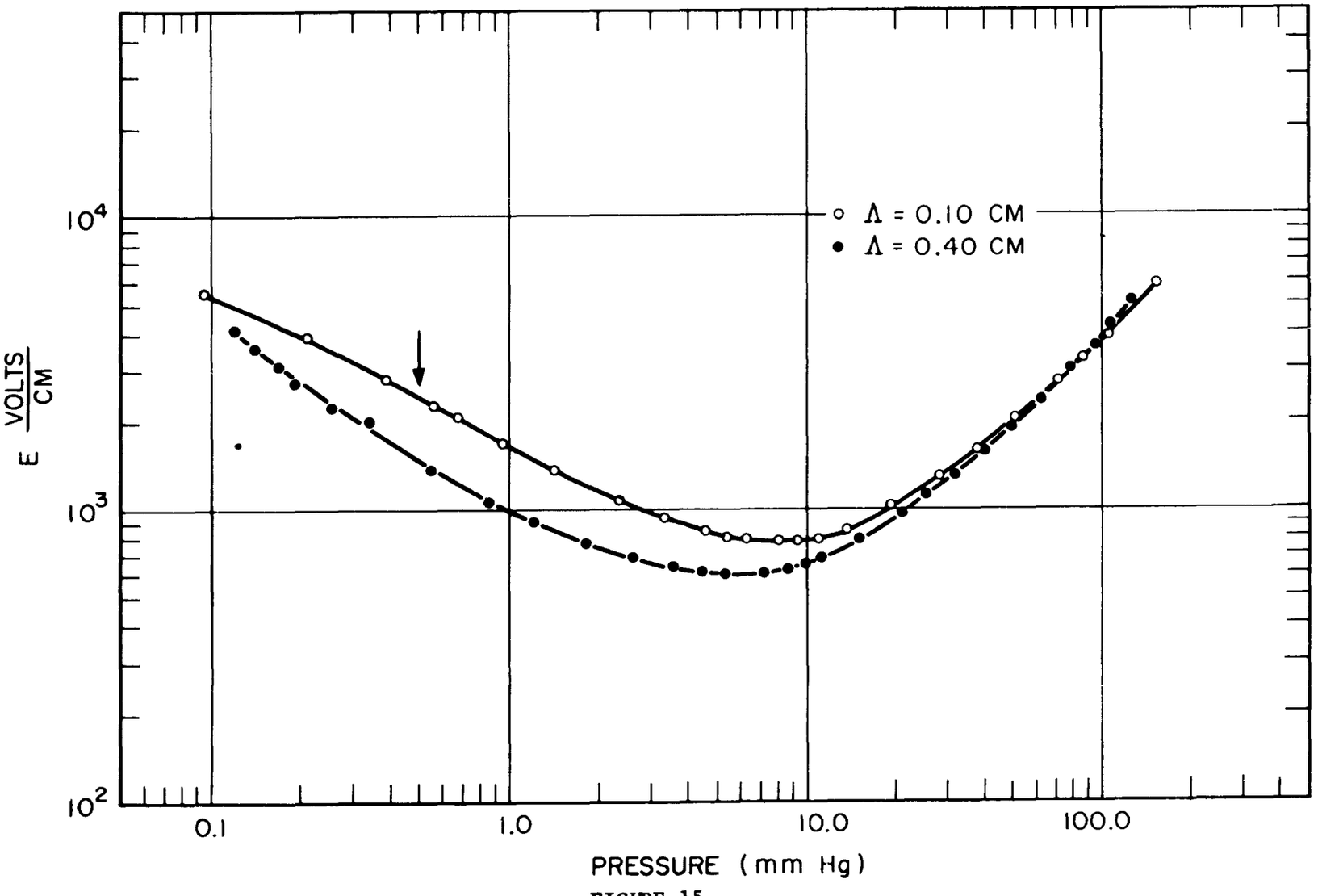

FIGURE 15

CW Breakdown Fields in Oxygen for Two Cavities
(f = 9.4 kMc/s)

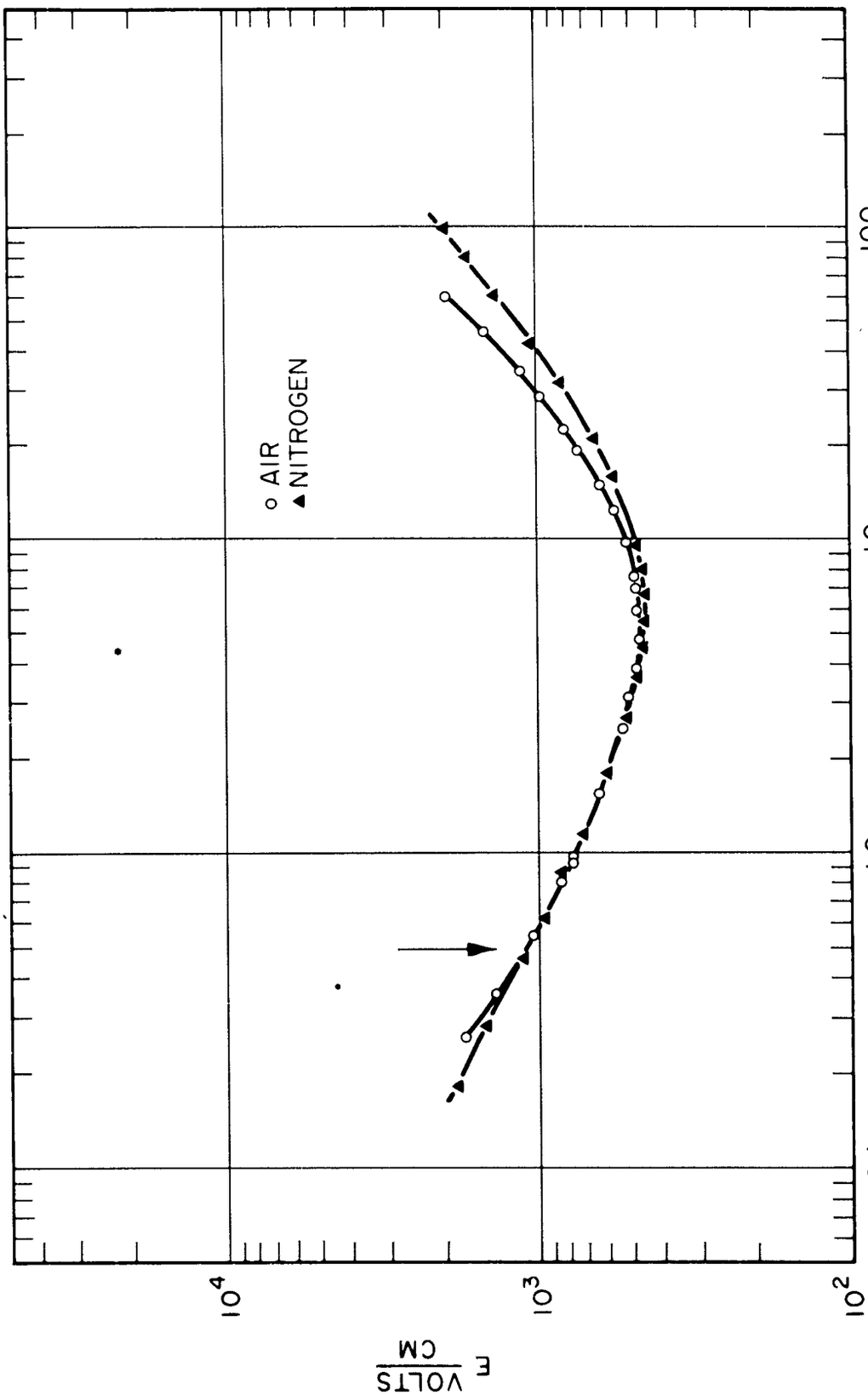

FIGURE 16

CW Breakdown Fields in Air and Nitrogen in a TM_{030} Cavity
(λ = 0.65 cm; f = 9.4 kMc/s)

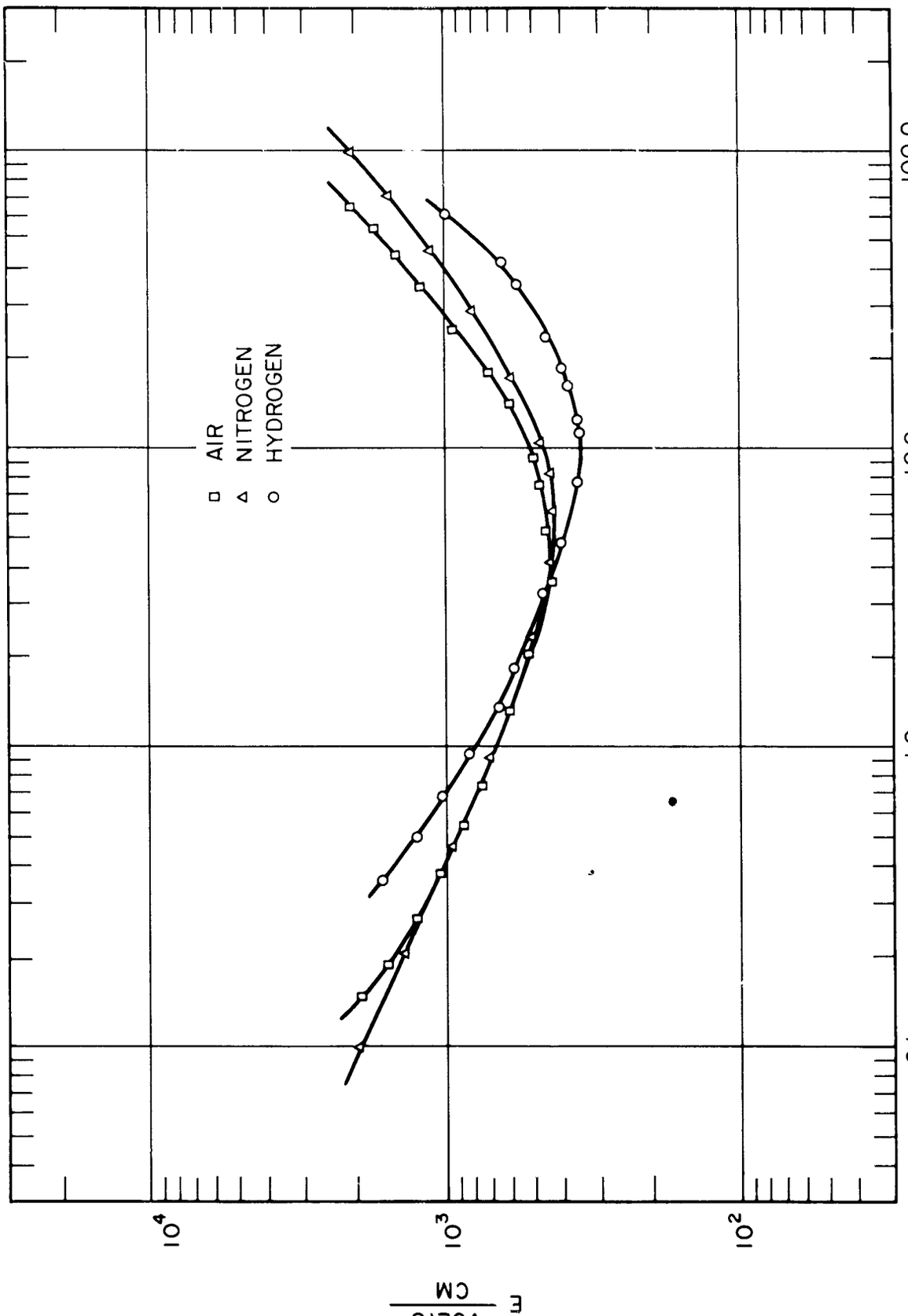

FIGURE 17

CW Breakdown in a TM_{030} Cavity in Air, Nitrogen, and Hydrogen (λ = 1.29 cm; f = 9.4 kMc/s)

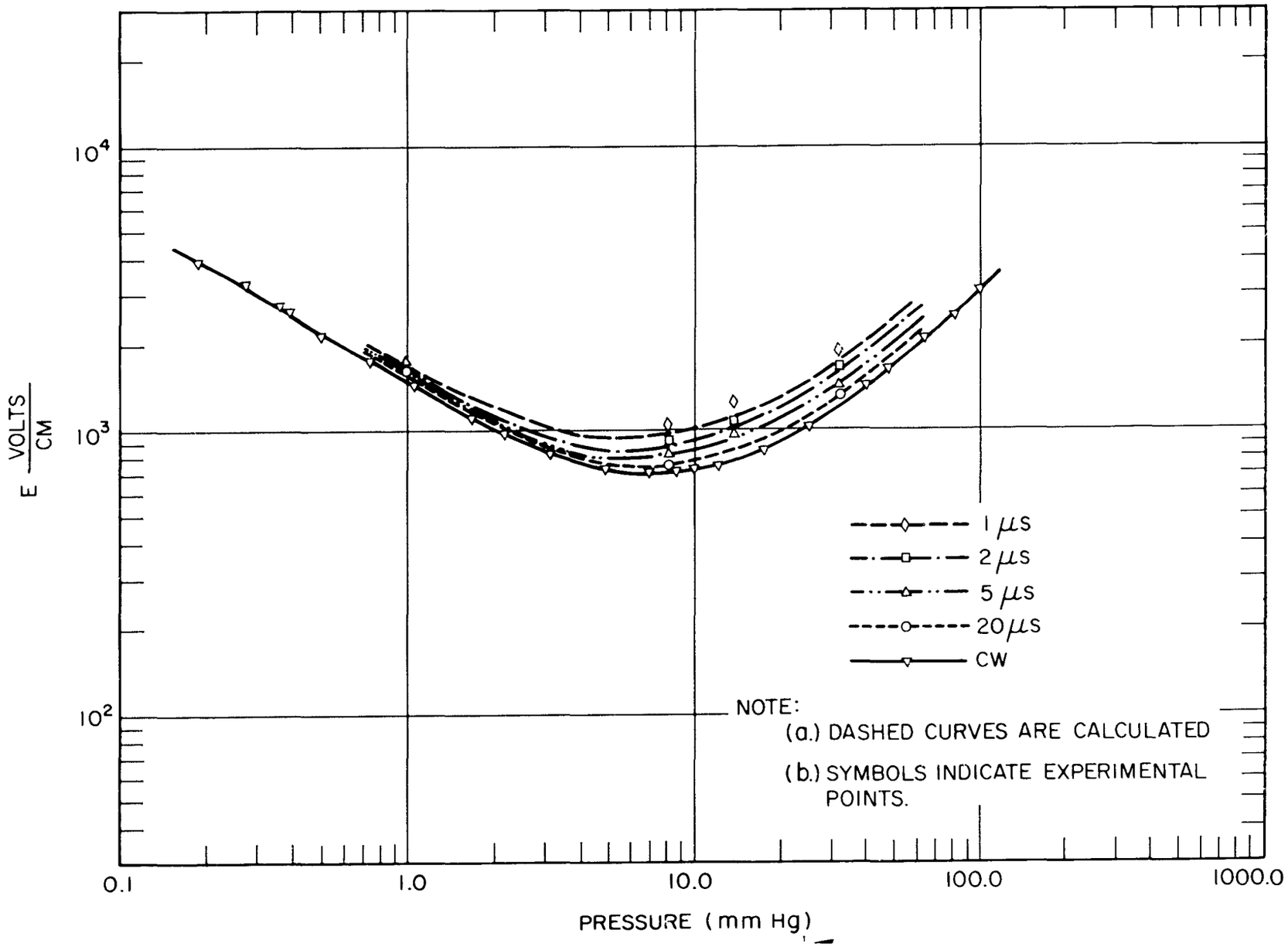

FIGURE 18

Pulsed Breakdown in Air
($\wedge$ = 0.10 cm; f = 9.3 kMc/s)

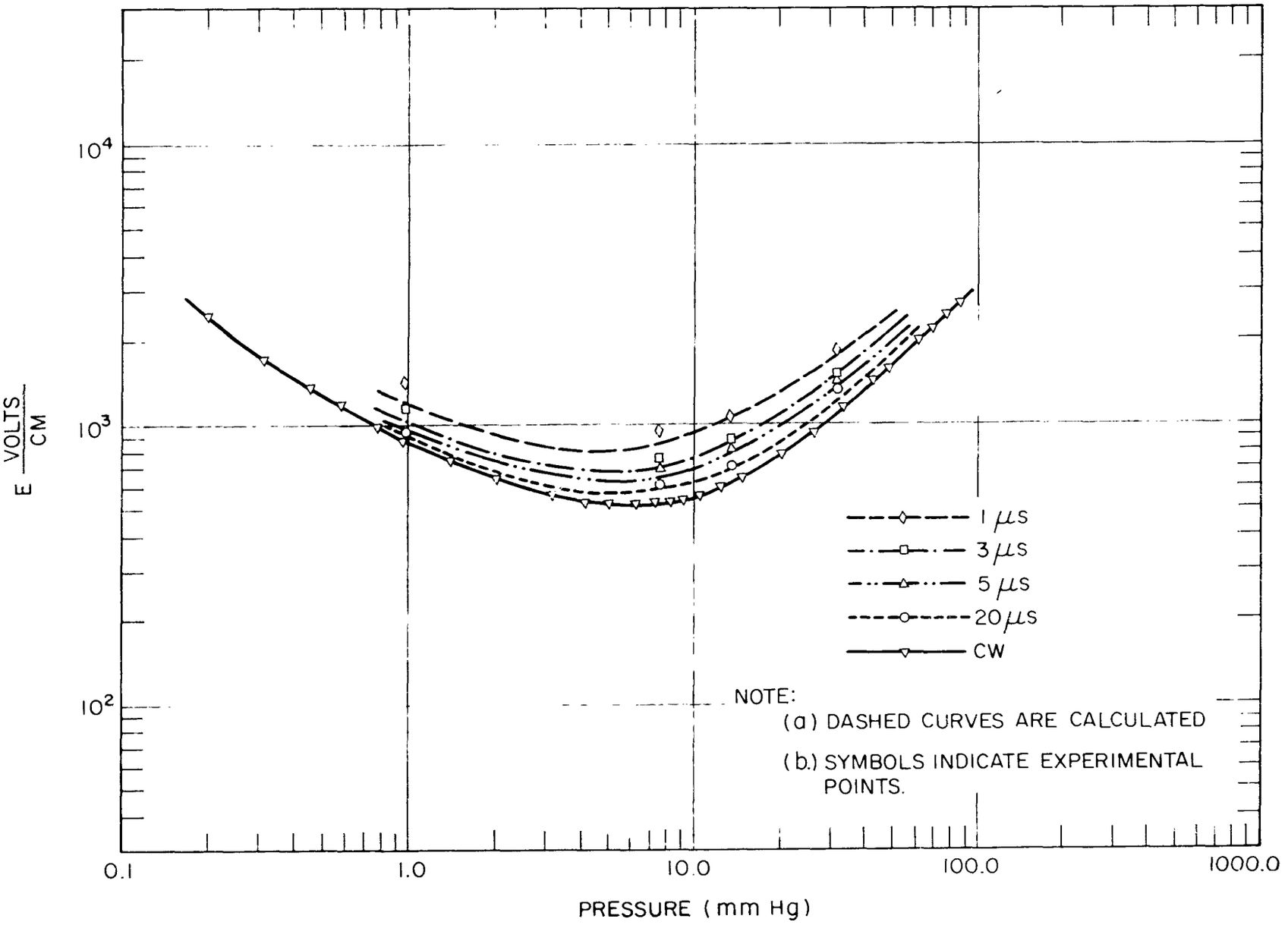

FIGURE 19

Pulsed Breakdown in Air
(λ = 0.40 cm; f = 9.3 kMc/s)

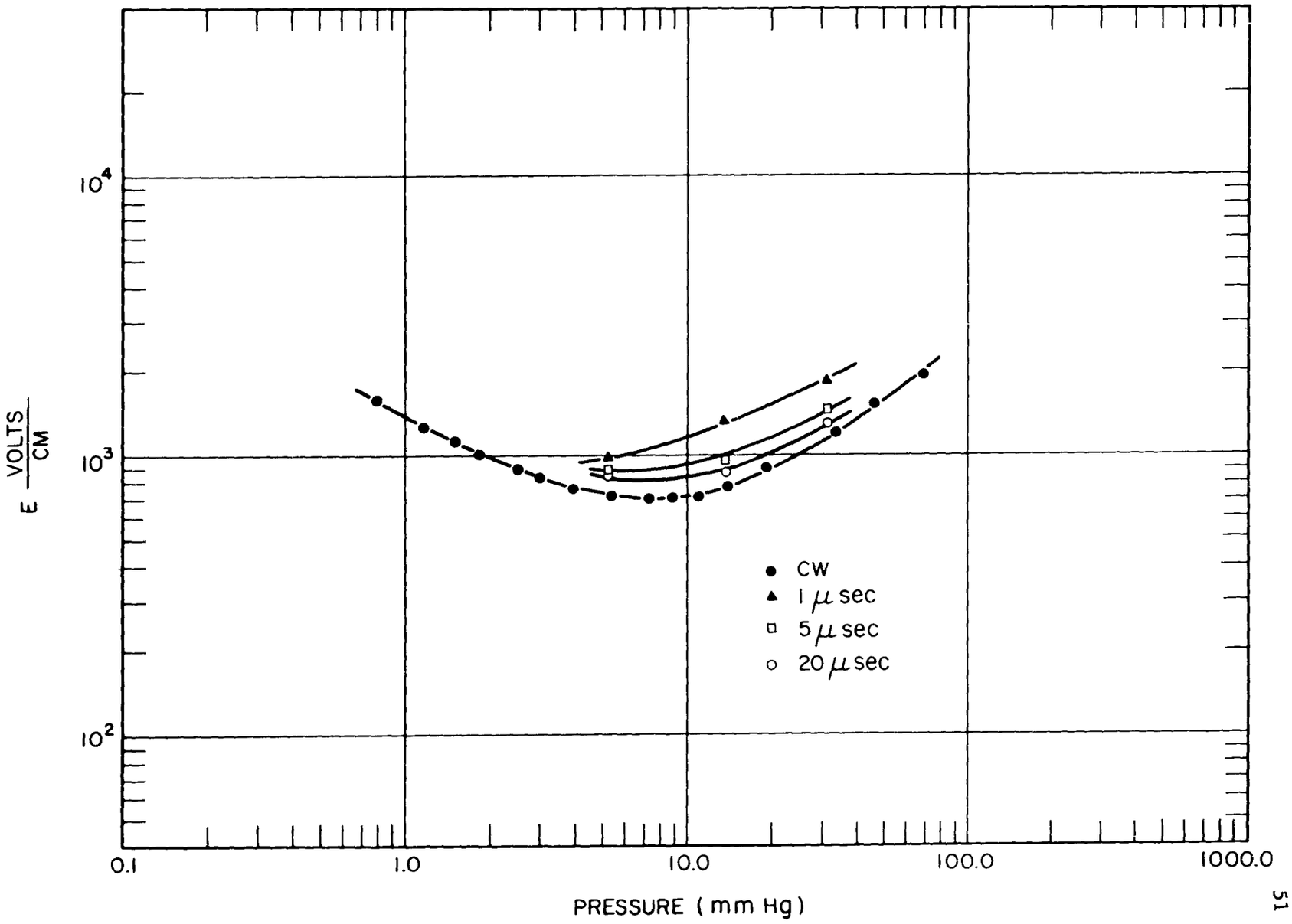

FIGURE 20

Pulsed Breakdown in Nitrogen
(λ = .103 cm; f = 9.3 kMc/s)

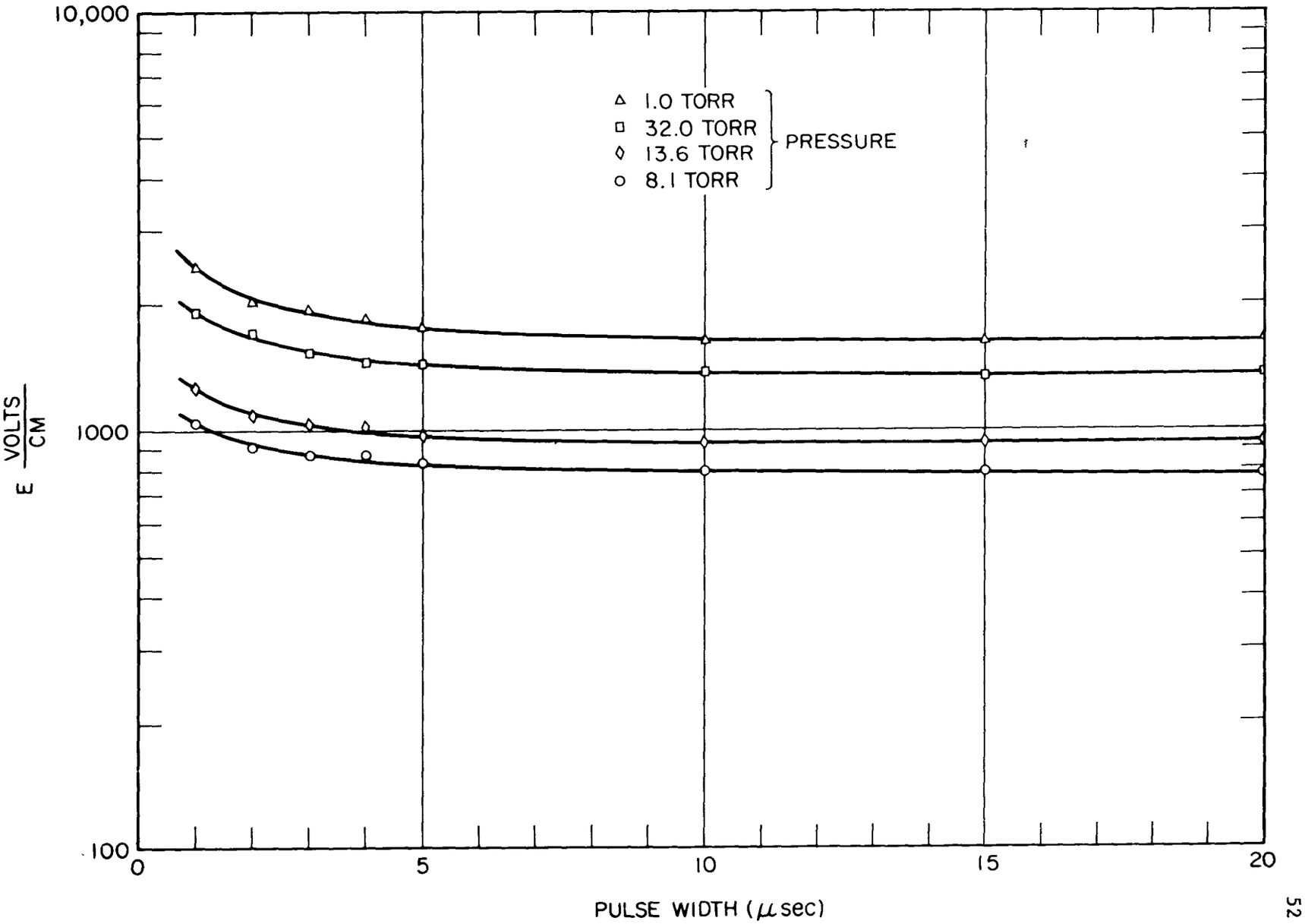

FIGURE 21

Pulsed Breakdown in Air as a Function of Pulse Width
(Λ = .10 cm; f = 9.3 kMc/s)

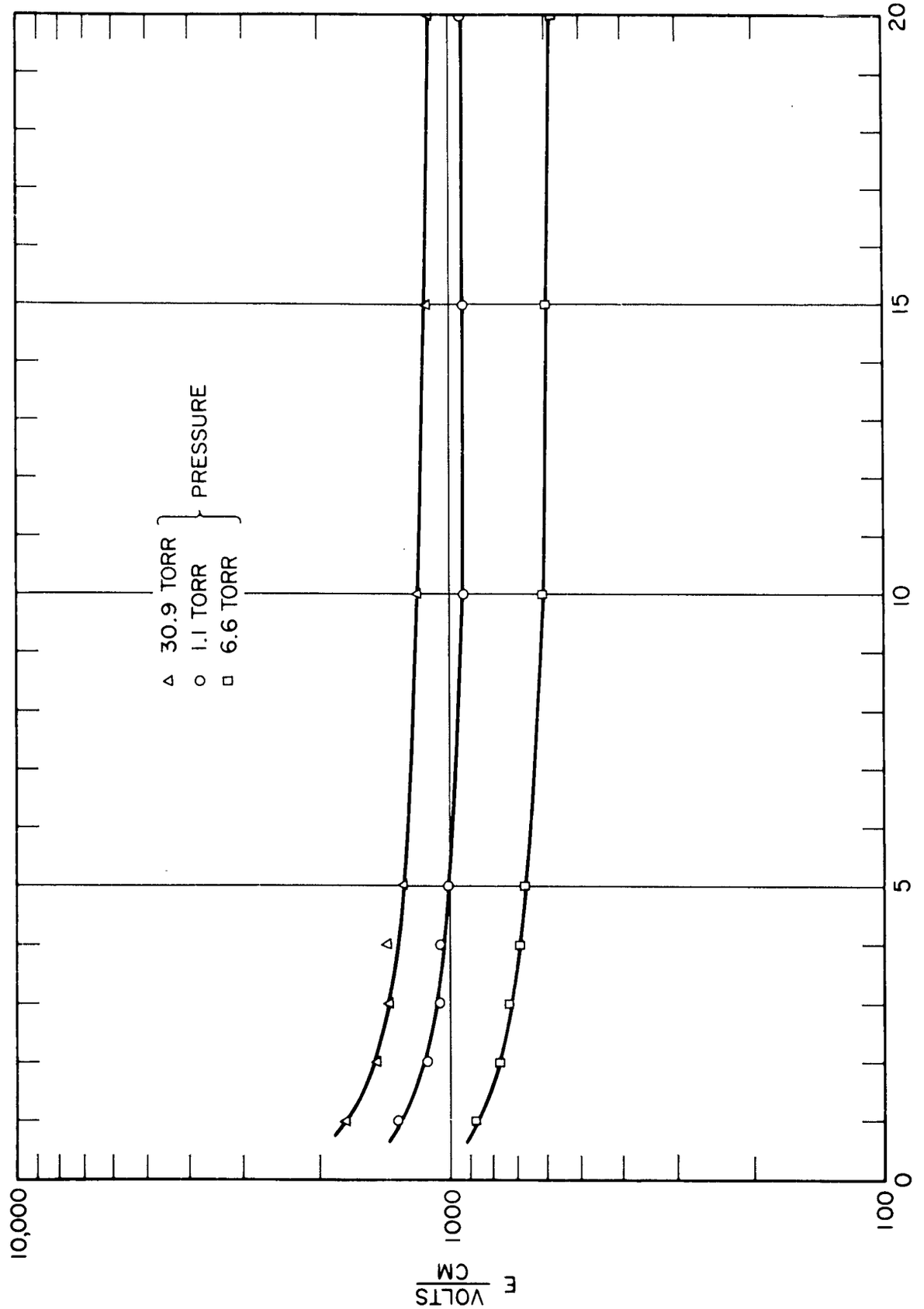

FIGURE 22

Pulsed Breakdown in Nitrogen as a Function of Pulse Width
(Λ = 0.40 cm; f = 9.4 kMc/s)

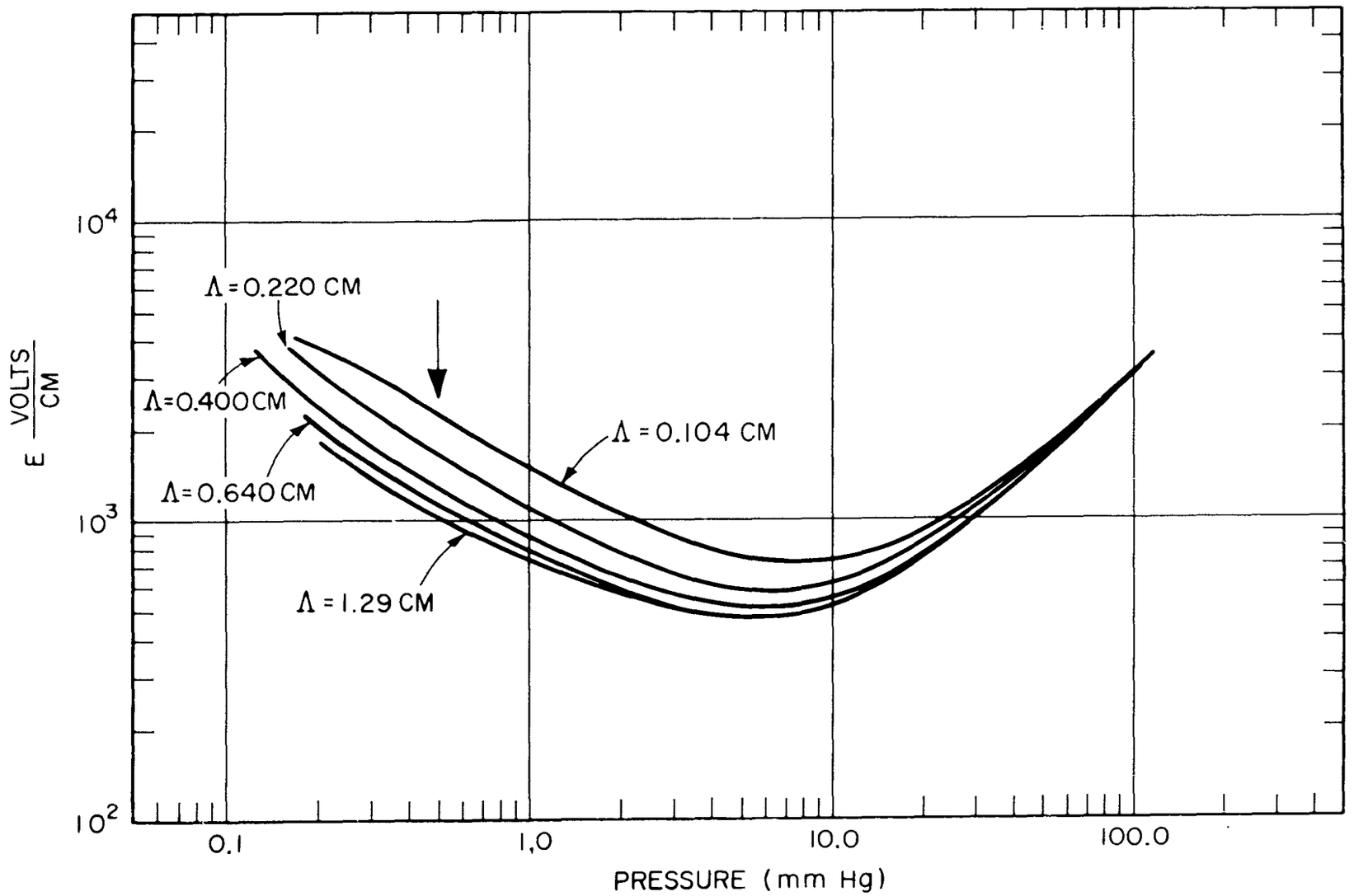

FIGURE 23

CW Breakdown in Air in Several Cavities
(f = 9.4 kMc/s)

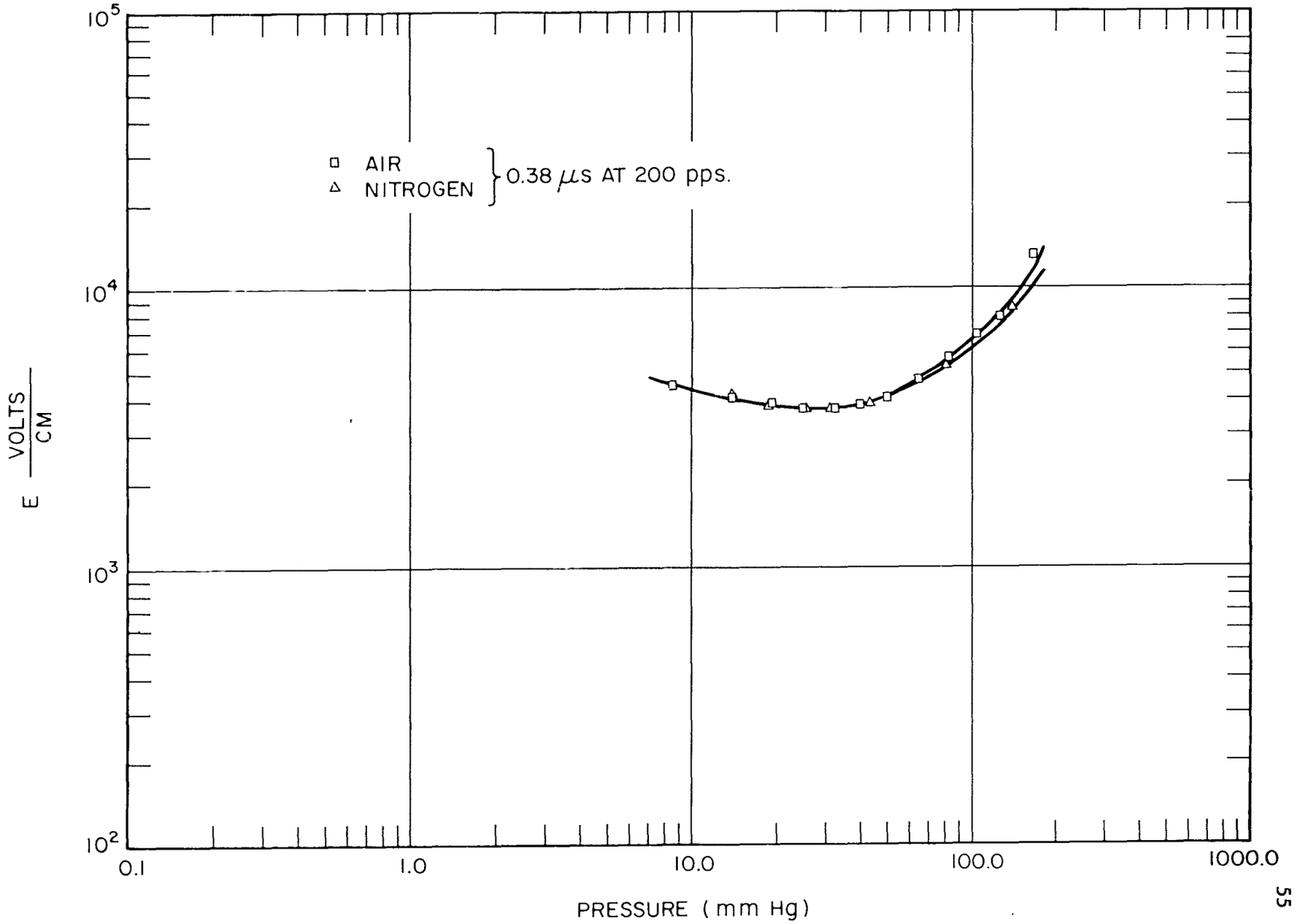

FIGURE 24

Pulsed Breakdown in Air and Nitrogen
(Λ = .09 cm; f = 24.1 kMc/s)

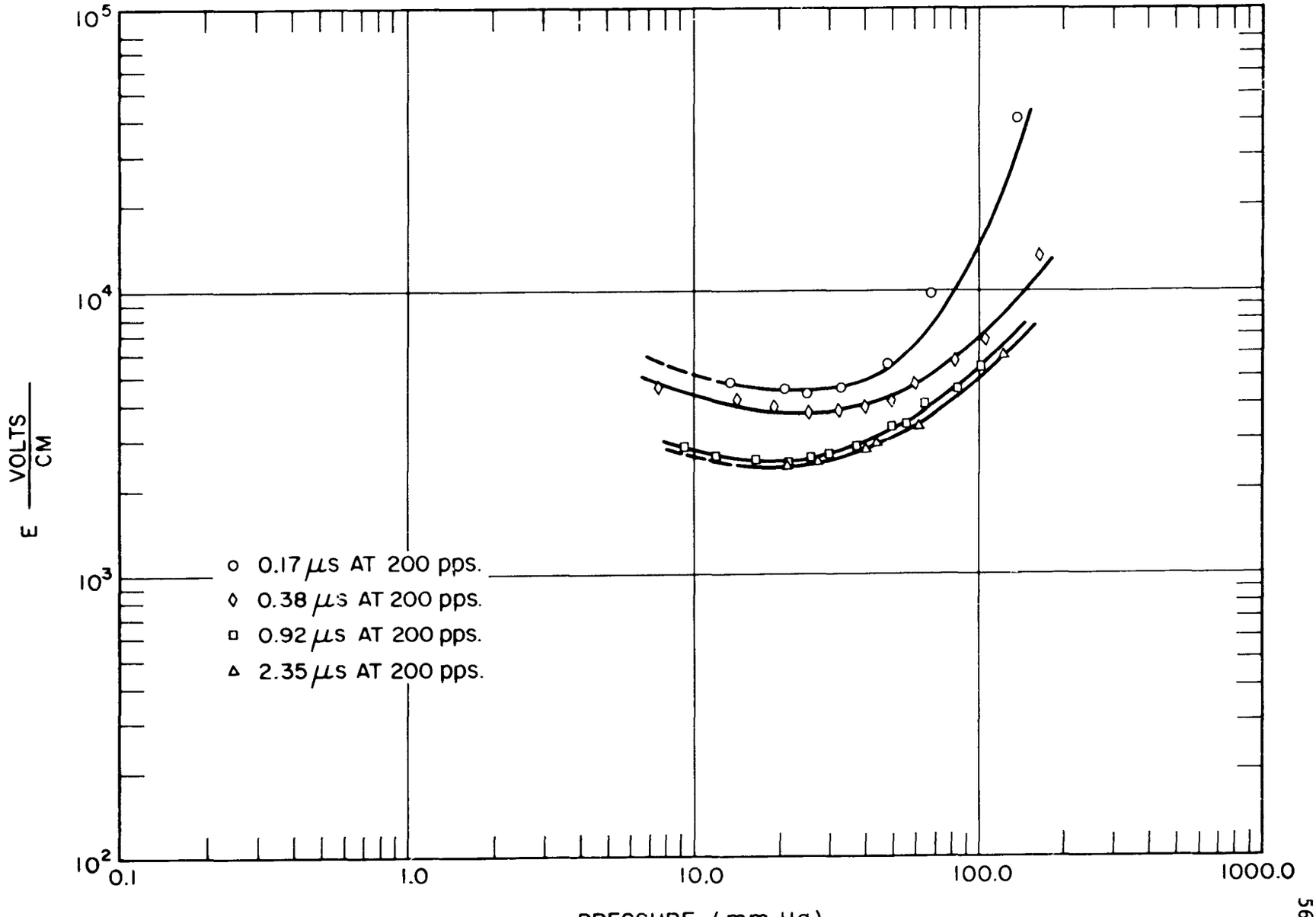

FIGURE 25

Pulsed Breakdown in Air
(Λ = .093 cm; f = 24.1 kMc/s)

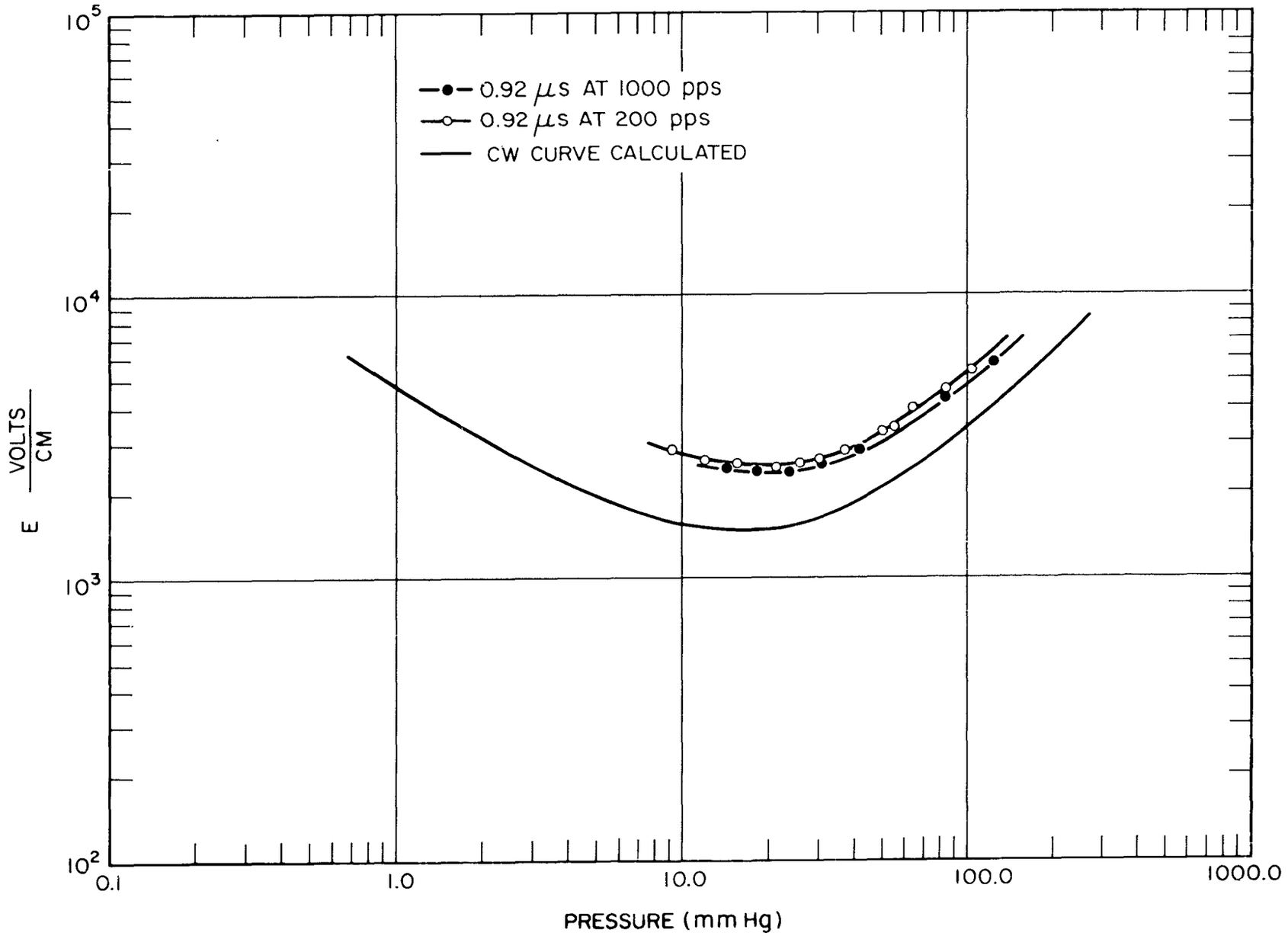

FIGURE 26

Pulsed Breakdown in Air at Different Repetition Rates
(Λ = .09 cm; f = 24.1 kMc/s)

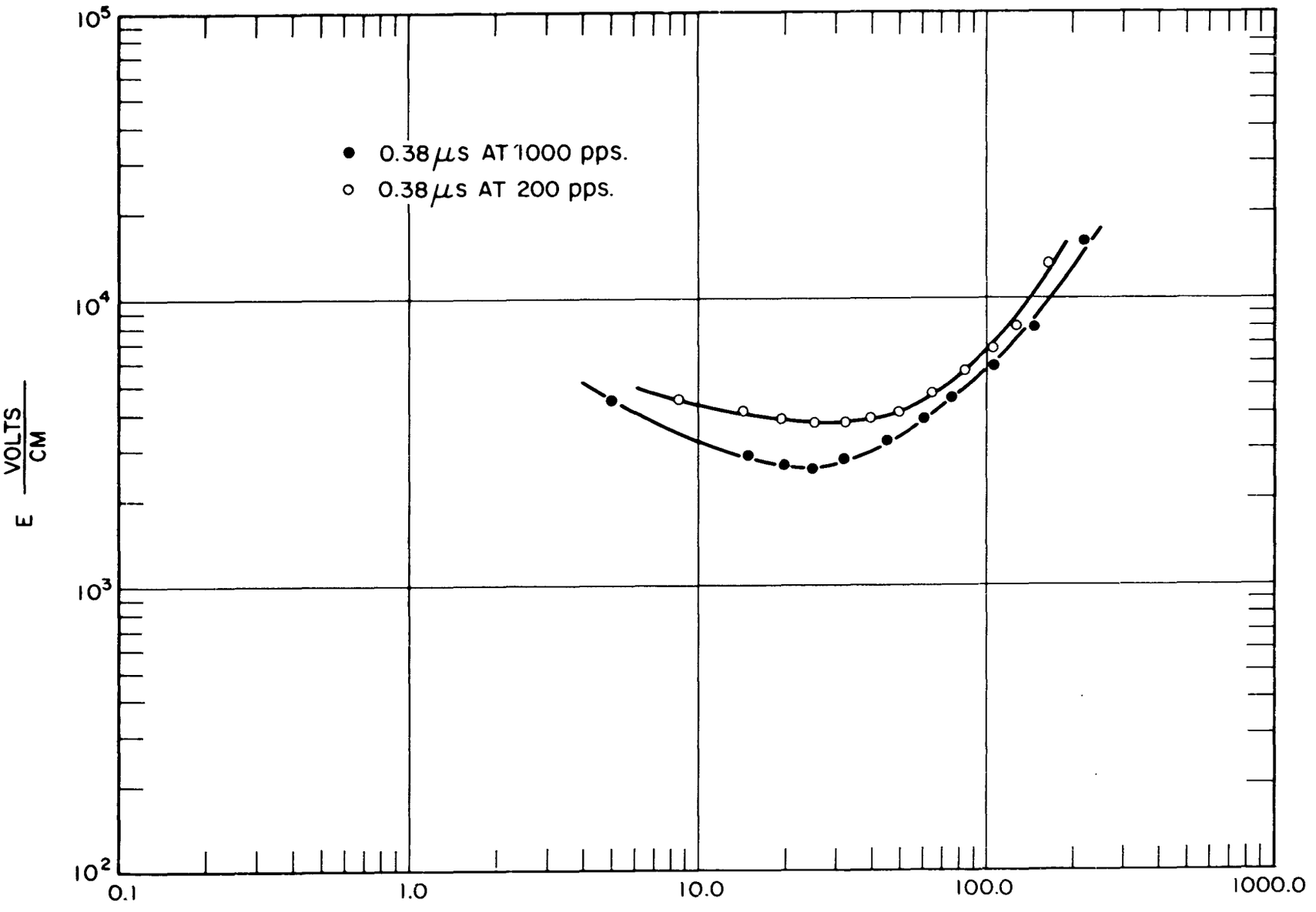

FIGURE 27

Breakdown in Air at .38 μs and Different Repetition Rates
(λ = .093 cm; f = 24.1 kMc/s)

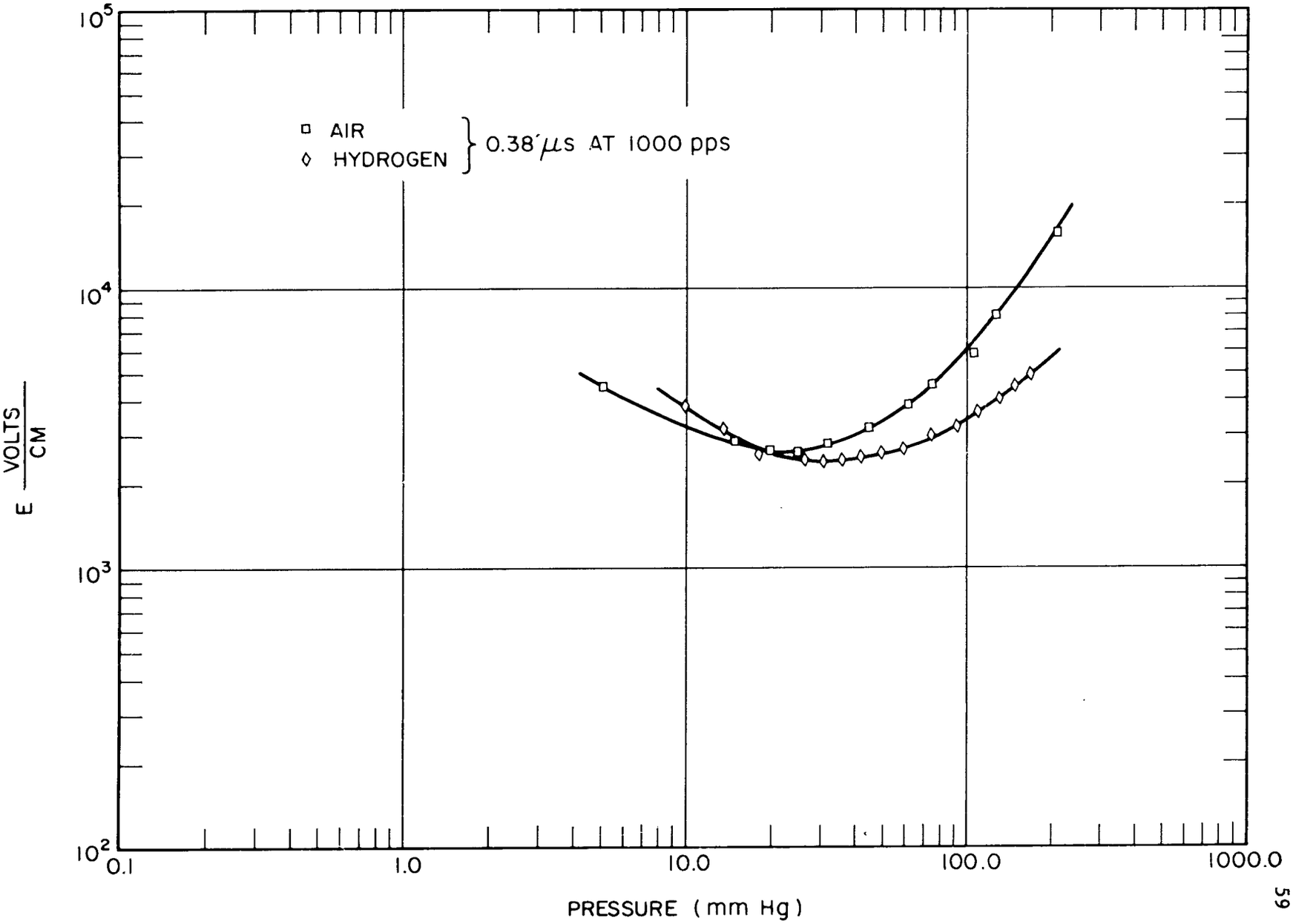

FIGURE 28

Breakdown in Air and Hydrogen at 24.1 kMc/s

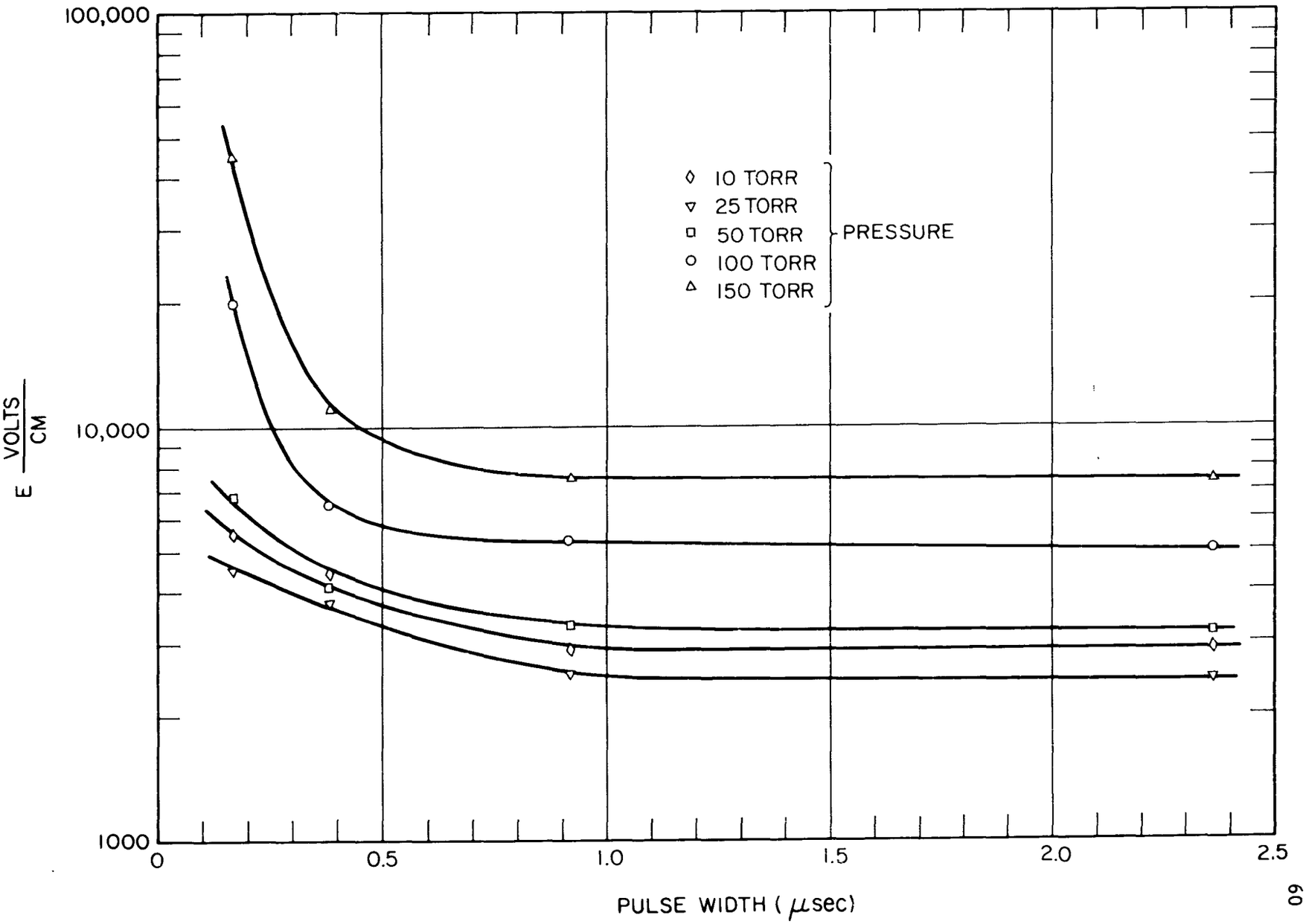

FIGURE 29

Breakdown in Air at 24.1 kMc/s as a Function of Pulse Width

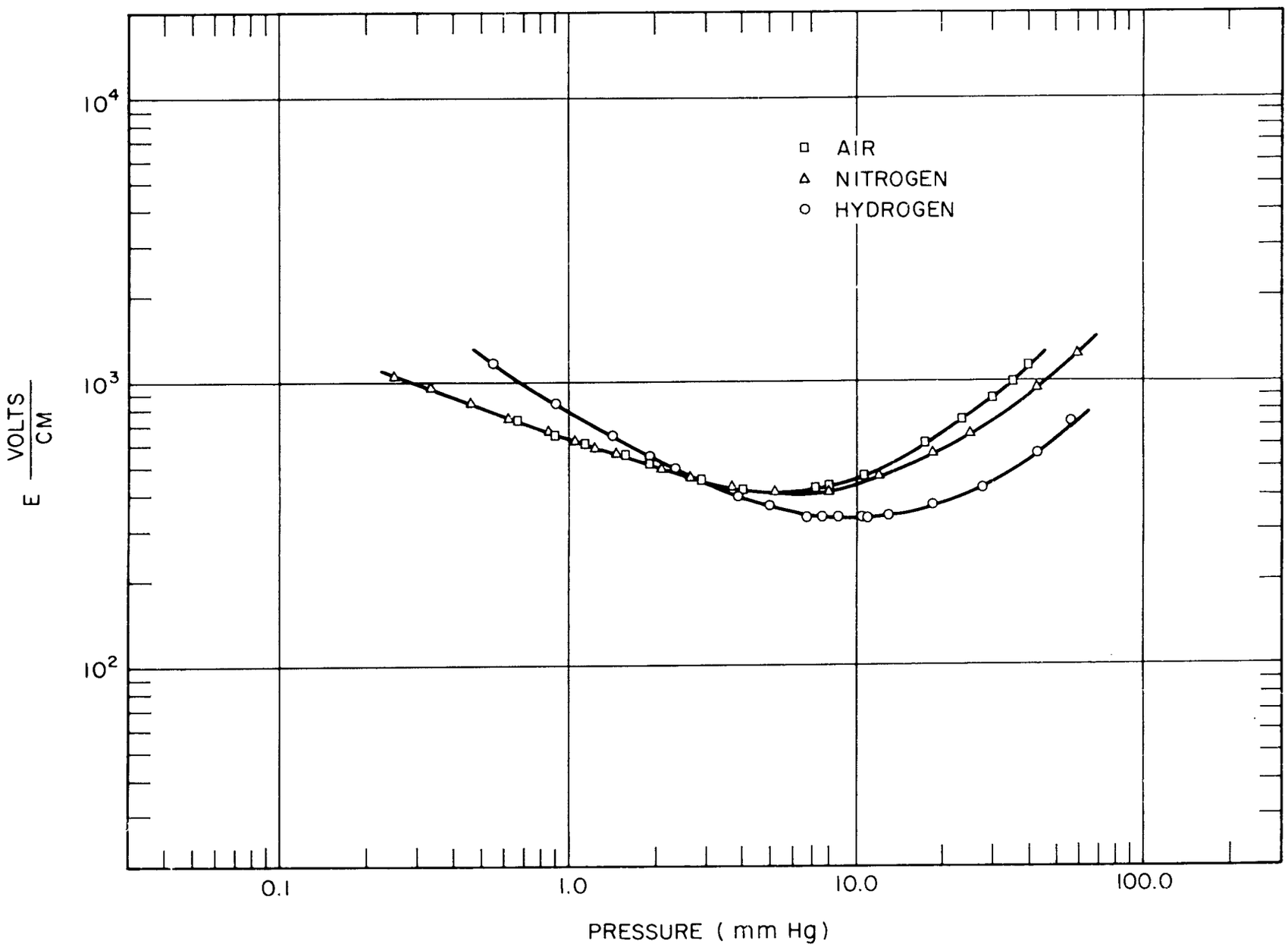

FIGURE 30

CW Breakdown in Air, Nitrogen, and Oxygen for a TM_{230} Cavity
(λ(theory) = .753 cm; λ(lowest mode) = 1.08 cm; f = 9.4 kMc/s)

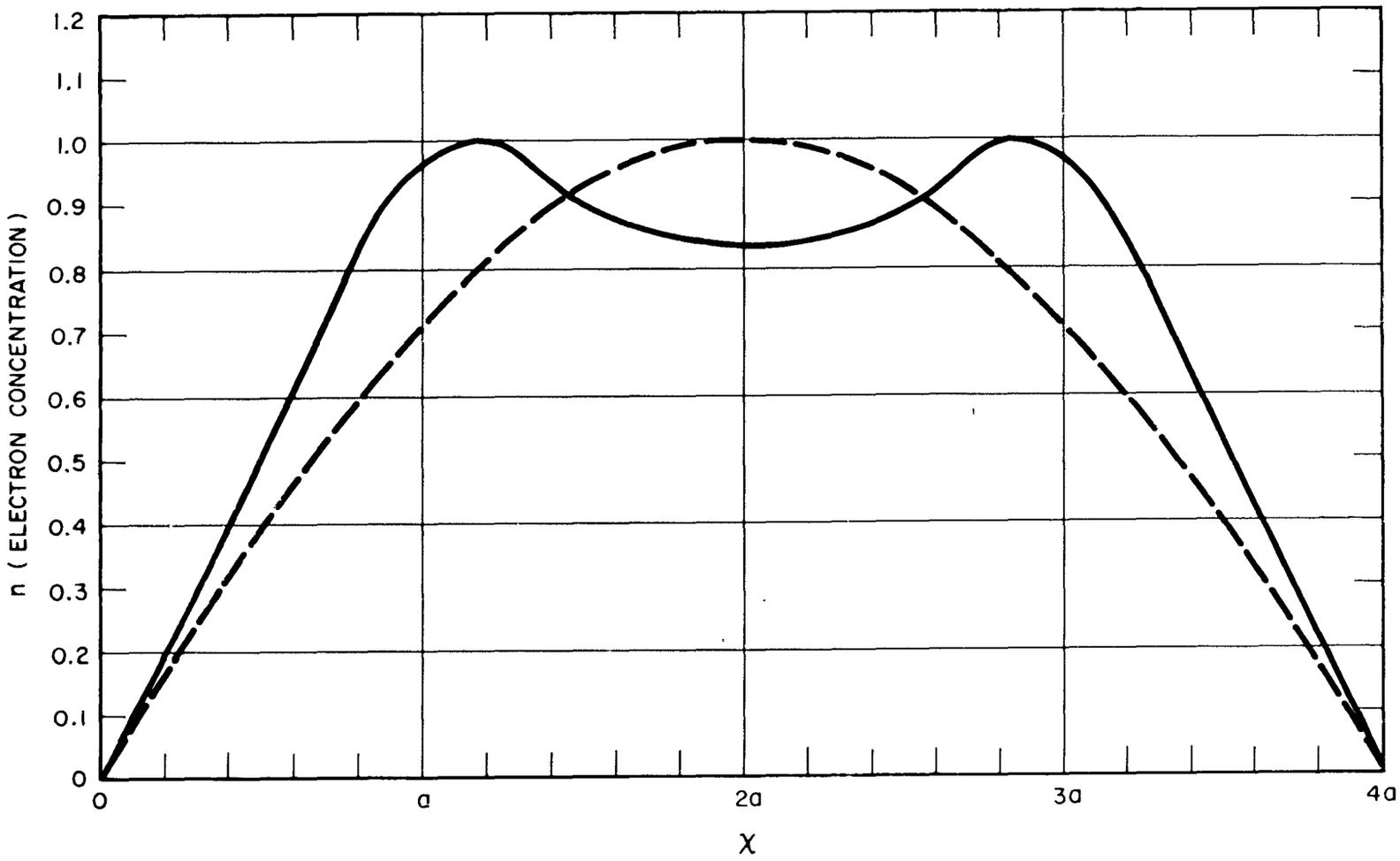

FIGURE 31

Electron Concentration Profile in TM_{230} Cavity

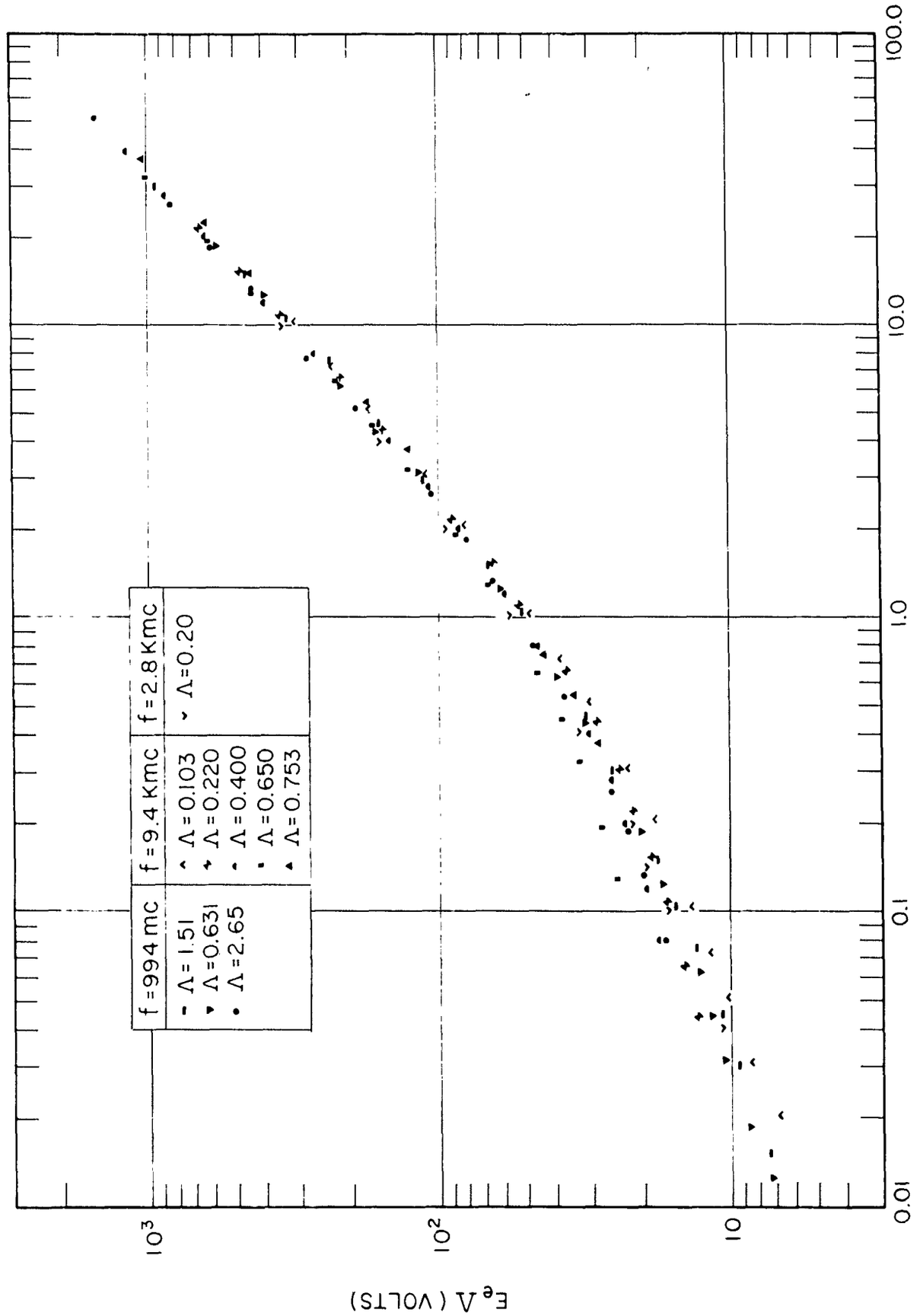

FIGURE 32

$E_e \Lambda$ as a Function of $p\Lambda$ for Several Cavities

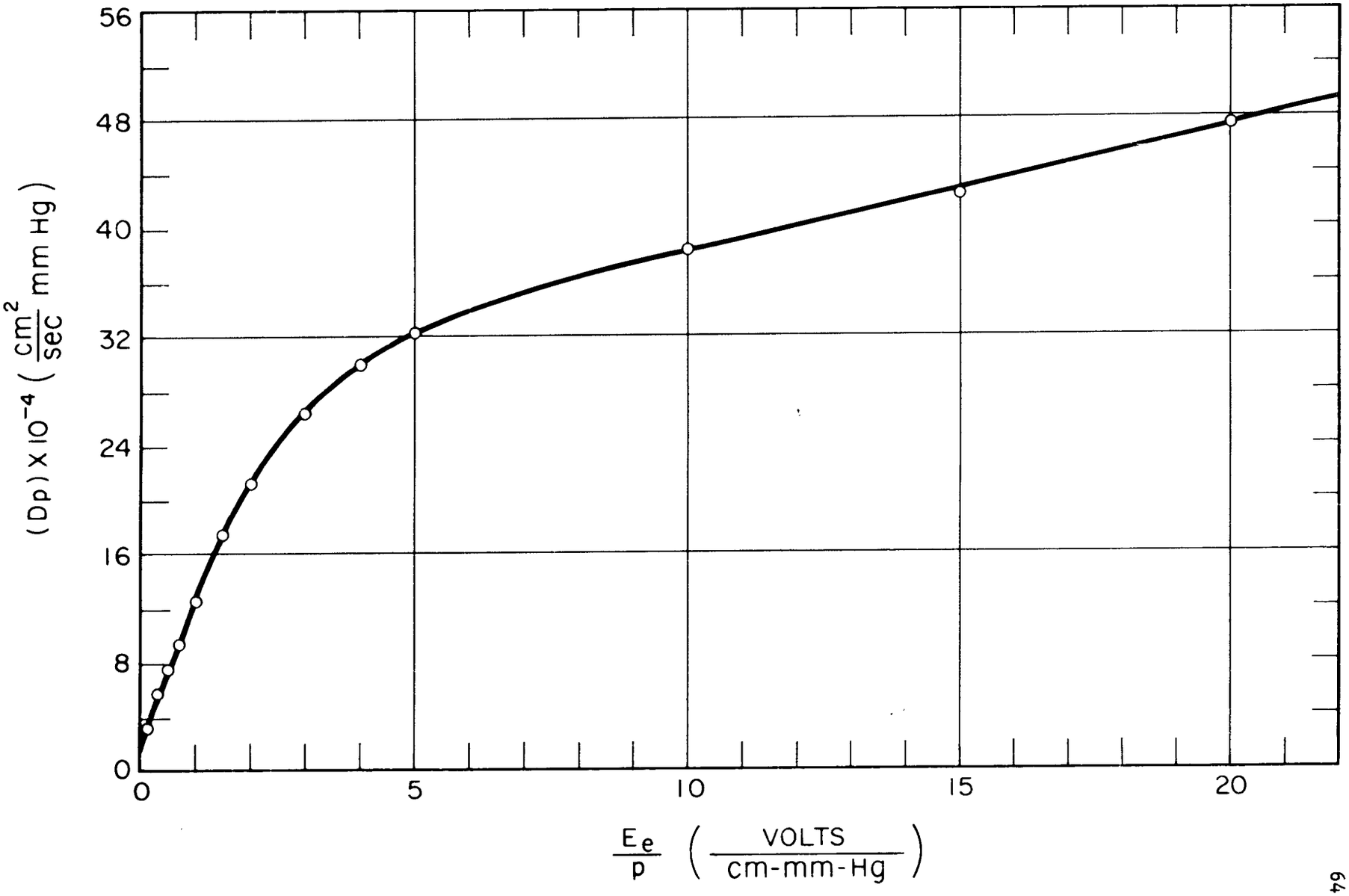

FIGURE 33

Diffusion Coefficient as a Function of E_e/p

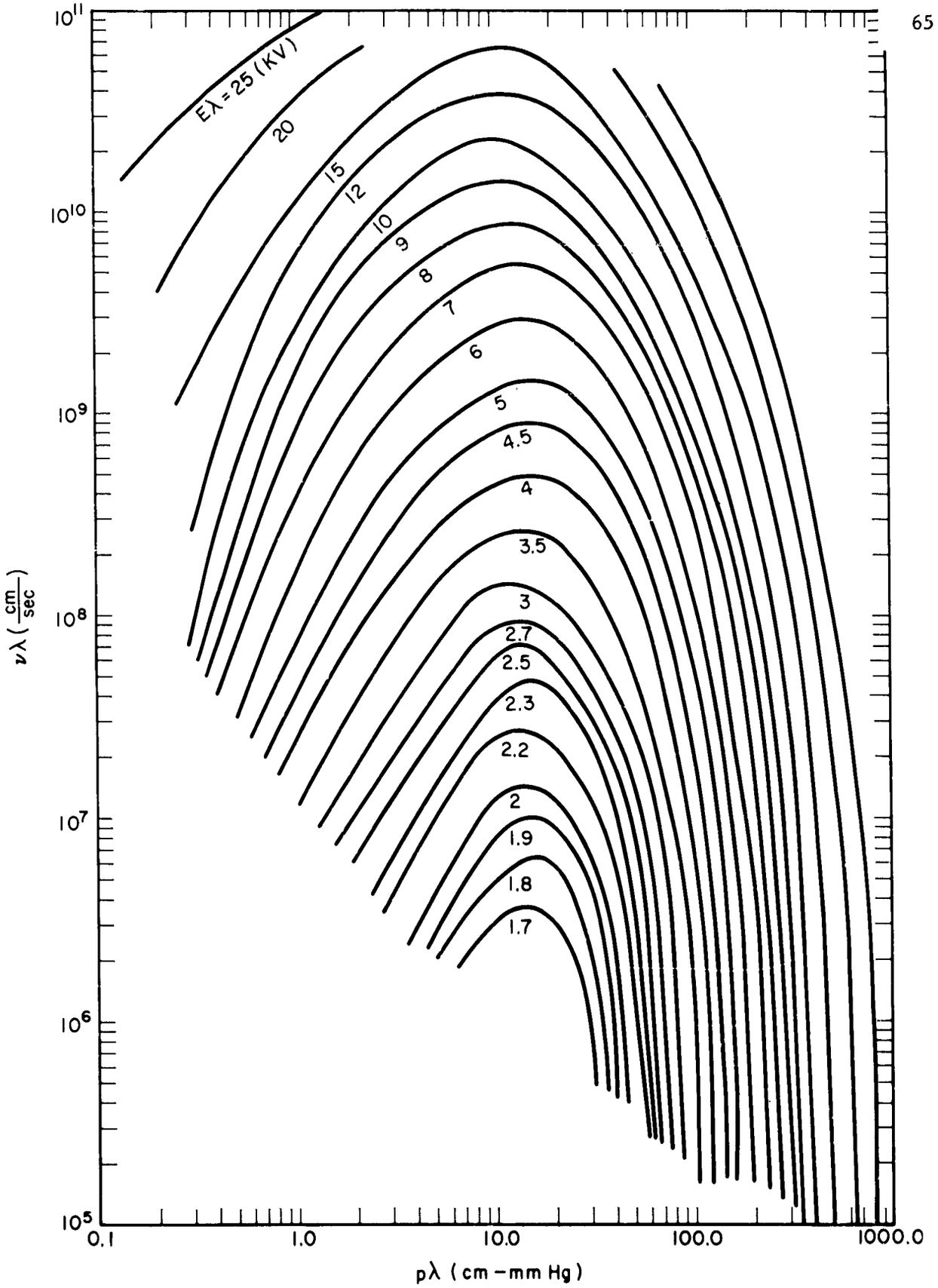

FIGURE 34

νλ as a Function of pλ for Constant Eλ

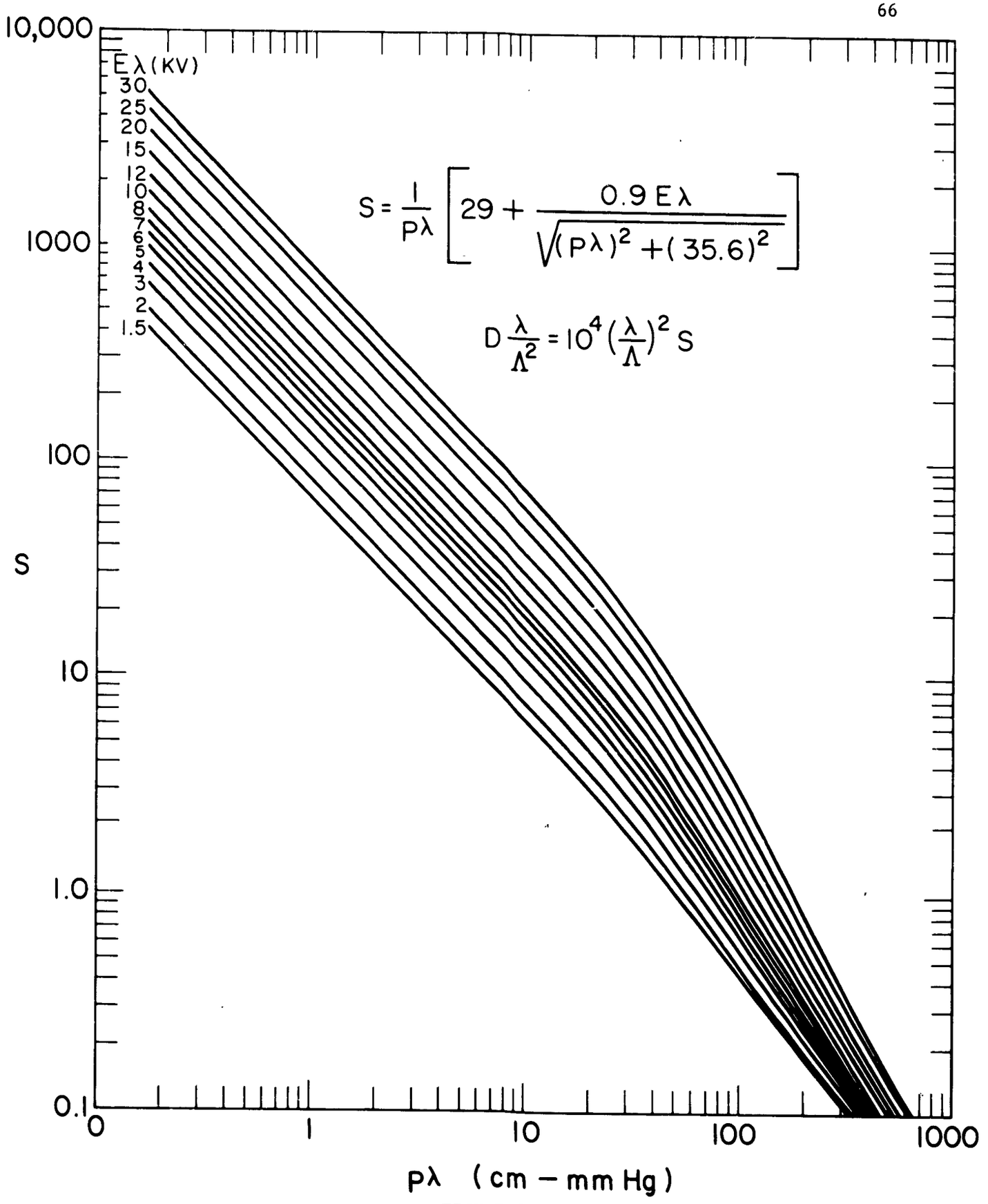

FIGURE 35

$D\lambda/\Lambda^2$ as a Function of $p\lambda$ for Constant $E\lambda$

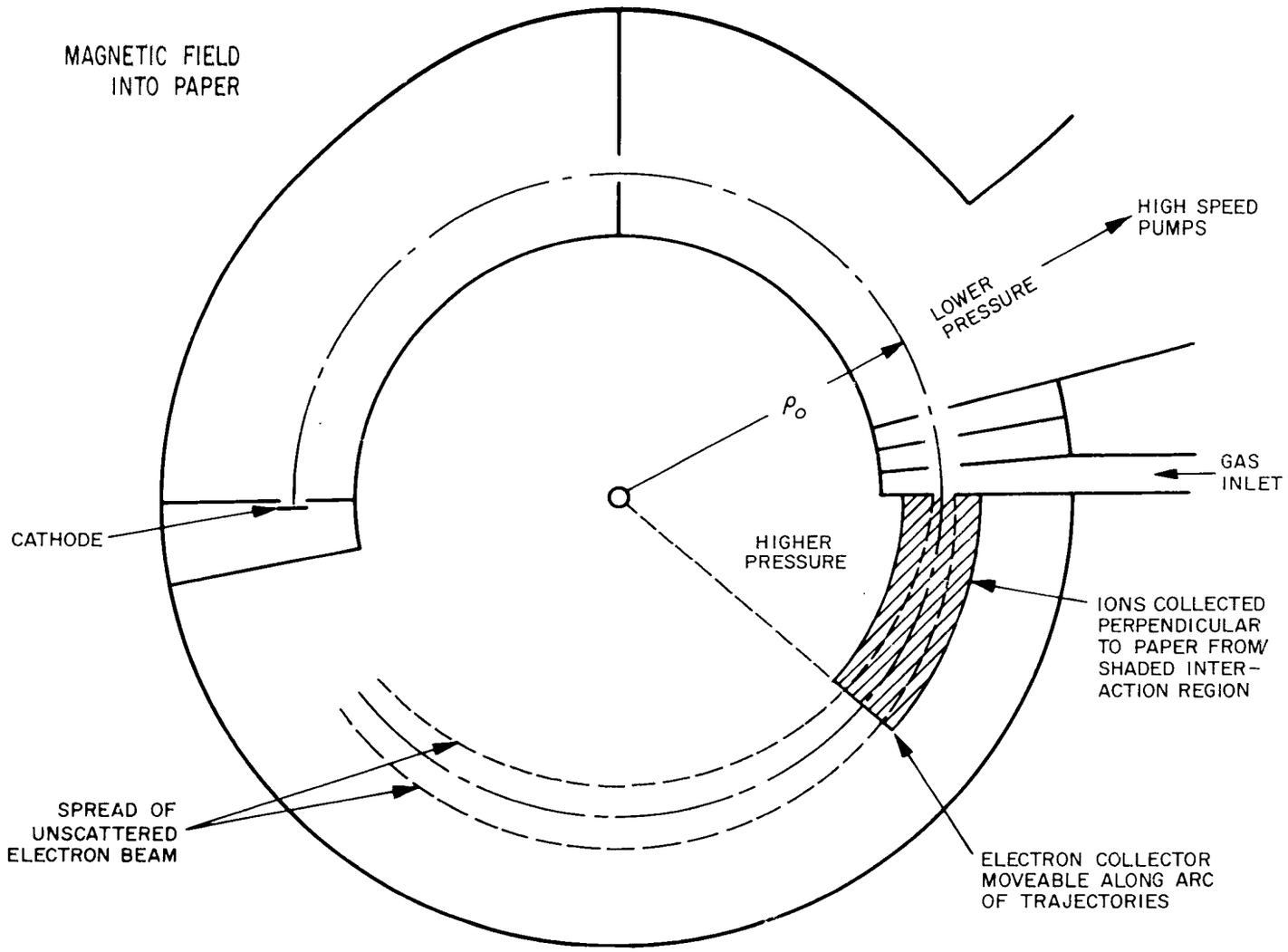

FIGURE 36

Schematic Diagram of Beam Scattering Apparatus